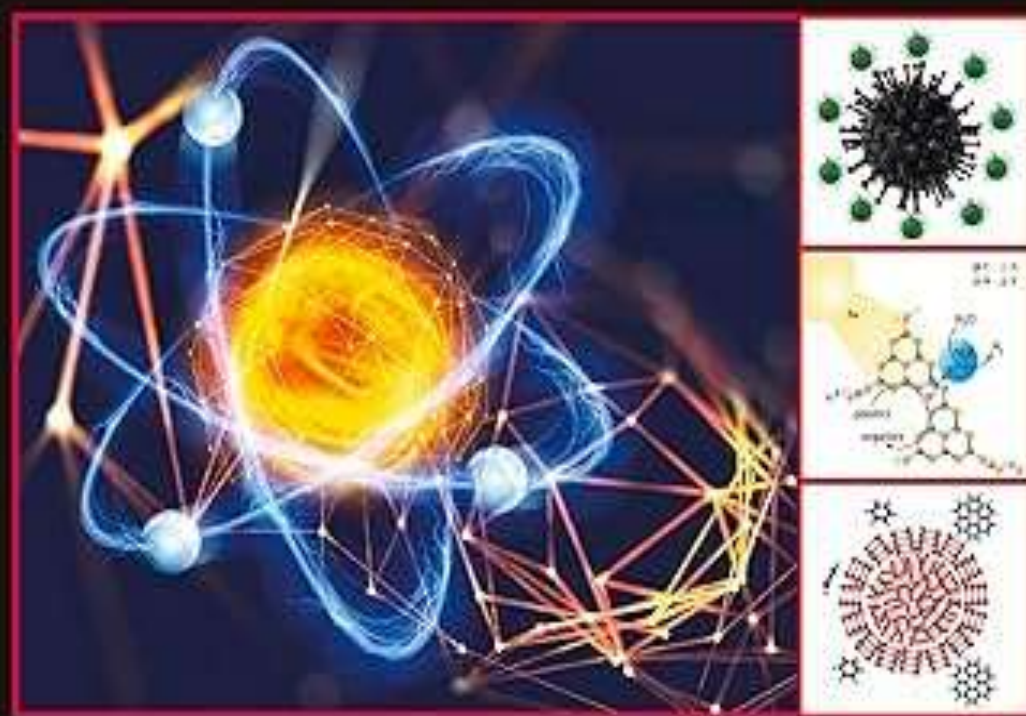


Progress in Biochemistry and Biotechnology

ADVANCES IN NANO AND BIOCHEMISTRY

Environmental and Biomedical Applications



Edited by
Pranay Pradeep Morajkar
Milind Mohan Naik



No. of pages: 618

Language: English

Edition: 1

Published: May 12, 2023

Imprint: Academic Press

Paperback ISBN: 9780323952538

eBook ISBN: 9780323952545

Table of contents

Cover image

Title page

Table of Contents

Copyright

Dedication and acknowledgment

Contributors

Preface

SECTION I. Environmental Studies

Chapter 1. Coupling of photocatalytic and bioremediation processes for enhanced mitigation of xenobiotic pollutants from wastewater

1.1. Introduction

1.2. Xenobiotic remediation methods

1.3. Challenges and future outlook

1.4. Summary and conclusion

Chapter 2. Bioinspired nanomaterials for remediation of toxic metal ions from wastewater

2.1. Introduction

2.2. Strategies for the bioinspired nanomaterials synthesis

2.3. Heavy metals removal technologies employing bioinspired nanoparticles

2.4. Conclusions and future prospect

Chapter 3. Biocompatible nanomaterials for sensing and remediation of nitrites and fluorides from polluted water

3.1. Introduction

3.2. Nitrites and fluorides in water and wastewater

3.3. Preparation techniques of bionanomaterials

3.4. Bionanomaterials as ionic sensors

3.5. Nitrites and fluorides remediation by bionanomaterials

3.6. Challenges and future perspectives

3.7. Conclusions

Chapter 4. Role of gum nanostructured hydrogels in water purification, desalination, and atmospheric water harvesting applications: Advances, current challenges, and future prospective

4.1. Introduction

4.2. Fundamental principles of techniques and instrumentation procedures

4.3. Latest research and development in the field

4.4. Summary and conclusion

4.5. Challenges and future outlook

Chapter 5. Versatile nanomaterials for remediation of microplastics from the environment

5.1. What are microplastics?

5.2. Effect of microplastics on human health

5.3. Traditional methods of microplastics separation

5.4. Advanced methods of microplastics separation

5.5. Nanomaterials

5.6. Remediation of microplastics using various nanomaterials

5.7. MPs adsorption strategies using nanomaterials

5.8. MPs degradation using nanomaterials

5.9. Limitations, challenges, and future outlook

Chapter 6. Plastic degradation—contemporary enzymes versus nanozymes-based technologies

6.1. Introduction

6.2. Major natural enzymes for plastic degradation

6.3. Major polymers that form plastic and their degradation

6.4. Nanozymes

6.5. Computational advancement for enzyme identification

6.6. Conclusion and future perspectives

Chapter 7. Current trends in sensing and remediation of gaseous pollutants in the atmosphere

7.1. Introduction to the gas phase chemistry and pollutants of the atmosphere (tropospheric emphasis)

7.2. Current trends in measurement approaches of important gaseous pollutants of the atmosphere and the associated challenges

7.3. Current trends in concentration levels and mitigation approaches

7.4. Challenges and future outlook

Chapter 8. Emerging nonnoble metal nanocatalysts for complete mitigation of combustion generated CO, NO_x, and unburnt hydrocarbons

8.1. Introduction

8.2. Different catalytic methods for the mitigation of pollutants emission

8.3. Latest research and development in mitigation of pollutants emission

8.4. Conclusion and future outlook

Chapter 9. Advanced methodologies for remediation of combustion-generated particulate matter (soot) from the environment

9.1. Introduction

9.2. Genesis of soot

9.3. Latest research and development in the remediation of combustion generated soot

9.4. Summary and conclusion

9.5. Challenges and future outlook

Chapter 10. Recent advances in quantification and remediation technologies for toxic PAH mitigation from the environment

10.1. Introduction

10.2. PAH detection and quantification technologies

10.3. Techniques for the environmental remediation of PAHs

10.4. Summary and future outlook

SECTION II. Biomedical Studies

Chapter 11. Application of nanoparticles as quorum quenching agent against bacterial human pathogens: a prospective therapeutic nanoweapon

11.1. General introduction

11.2. Nanoparticles: fundamentals and principles

11.3. Latest research on nanoparticles as quorum quenching agents

11.4. Mechanisms of quorum quenching by nanoparticles

11.5. Techniques and biosensors involved in quorum quenching research of nanoparticles

11.6. Summary and conclusion

11.7. Challenges and future prospects

Chapter 12. Biocompatible green-synthesized nanomaterials for therapeutic applications

12.1. Introduction

12.2. Fundamental principles of techniques and instrumentation/methods/procedures involved

12.3. Latest research and development in the field

12.4. Summary and conclusion

12.5. Challenges and future outlook

Chapter 13. Toxicological aspects of nanomaterials in biomedical research

13.1. Introduction

13.2. Toxicity of nanomaterials in biomedicine

13.3. Genotoxic biomarkers

13.4. Safety against toxic effects

13.5. Summary and conclusions

13.6. Challenges and future outlook

Chapter 14. Quantum dots and hybrid structures as an innovative solution for bioimaging and diagnosis of viral infections

14.1. Introduction

14.2. Synthesis methods, modification strategies, and properties of QDs

14.3. QDs photoluminescence—principles/mechanisms

14.4. Application of QDs in bioimaging and detection of viruses

14.5. Challenges and future prospects

14.5. Challenges and future prospects

14.6. Summary and conclusion

Chapter 15. Magnetic nanomaterials and their hybrids for magnetic hyperthermia

15.1. Introduction

15.2. Nanomagnetism

15.3. Magnetic alloy nanoparticles for MHT

15.4. Ferrite magnetic nanoparticles for magnetic hyperthermia

15.5. Superparamagnetic materials for magnetic hyperthermia

15.6. Summary and conclusion

15.7. Challenges and future outlook

Chapter 16. Advanced functionalized nanomaterial-based electrochemical biosensors for disease diagnosis

16.1. Introduction

16.2. Fundamental techniques of biosensing and nanomaterial-based diagnostic tools

16.3. Latest research and development in the biosensing field

16.4. Conclusion and future perspectives

Chapter 17. Recent advances in MOFs-based nanocomposites for treatment of retinopathy or retina-related biomedical applications

17.1. Introduction

17.2. Traditional methods of drug loading for ocular disease treatment

17.3. Categories of nanocarriers

17.4. Drug delivery routes for nanocarriers

CHAPTER 1

Coupling of photocatalytic and bioremediation processes for enhanced mitigation of xenobiotic pollutants from wastewater

Sarvesha S. Shetgaonkar, MSc¹, Amarja P. Naik, PhD¹, Milind M. Naik, PhD² and Pranay P. Morajkar, PhD¹

¹School of Chemical Sciences, Goa University, Taleigao, Goa, India;

²School of Biological Sciences and Biotechnology, Goa University, Taleigao, Goa, India

1.1 Introduction

Recent development in the industrial and agricultural sectors has upgraded the quality of human life but at the same time it has led the world into a cancerous grip of environmental pollution [1]. Various industries such as textile, fertilizer, food processing, paper, cosmetics, leather, etc., directly discharge their waste effluents (containing xenobiotics) into water bodies which severely affects the aquatic and human life [2]. Xenobiotic means “foreign to life” are synthetic chemical compounds including azo dyes, pesticides, polychlorinated biphenyls (PCBs), chlorinated solvents, and antibiotics, which enter into the biological environment and cause detrimental effects on biota.

Azo dyes are organic contaminants containing azo group ($-N=N-$), aromatic rings, and extended π -conjugation which allows the molecule to absorb visible radiation [3]. They are frequently being used and discharged into natural water bodies by various textile, leather, and food processing industries. Dyes such as Amaranth, Rhodamine B, and Methyl orange, persist into the environment unaltered due to their complex aromatic structure, photo stability, low biodegradability. Hence, they pose adverse effects on human health in terms of genotoxicity and carcinogenicity [4]. Pesticides are another important class of xenobiotics. Pesticides, especially herbicides, insecticides, and fungicides are extremely useful in domestic, agricultural, and industrial areas for destroying, controlling, and combating pests such as ticks, rats, insects, bugs, etc. [5]. Nevertheless, they have played a major role in development of agricultural sector by increasing the yield of crops by protecting them from pest attack. However, excessive use and untreated disposal of these recalcitrant chemicals has led to its accumulation in the environment. One of the major drawbacks of pesticides is that along with the target species (pests) it also affects the nontarget species (including humans) which further leads to ecological imbalance in the natural ecosystem. Pesticides can be further

classified into herbicides (Carbamates), insecticides (Organo-phosphorous compounds), and fungicides (Chloro-pyridines) [6]. Organophosphorus pesticides act as depressive chemicals, retard insulin production, and cause malfunctioning of nutrients. Carbamate pesticides are found to weaken the immune system, affect the working of mitochondria, and cause reproductive and neurological disorders [7]. Chloro-pyridines are known to cause fatty liver degeneration. Further, impaired vision, headache, lack of coordination, problem in breathing, and fall in heartbeat are some of the other harmful effects of pesticides [8]. Also, upon long-term exposure to pesticides one may experience skin allergies along with sneezing, rashes, cough, asthma, and blisters.

PCBs are polyaromatic chlorinated organic compounds which differ in chlorine numbers and positions. About 370,000 tons of PCBs are produced globally, out of which ~31% are being released into the environment [9]. Ever since their introduction decades ago, PCBs have been widely used as hydraulic fluids, solvent extenders, heat transfer fluids, plasticizers, dielectric fluids, and flame retardants [10]. Owing to their insulating and nonflammable properties, PCBs also find application as lubricants and coolants in transformers, capacitors, etc. PCBs are also utilized in sealants, paints, polyvinylchloride (PVC), adhesive, and pressure-sensitive copy paper. However, PCBs were banned in 1970s due to their persistence and toxicity [11]. Like any other xenobiotics, PCBs are known to severely affect our immune, endocrine, reproductive and nervous systems due to bioaccumulation through food chain. In the past, the main reason for release of PCBs into the environment was its improper transport, storage, and disposal problems [10]. Recent studies have also shown that PCBs in soil also affect the living organisms of soil thereby making the soil lose its productivity [9].

In general, xenobiotics (azo dye, pesticides, and chlorinated compounds) contain structural elements which are not of natural occurrence, as they are industrially prepared. Natural microorganisms previously had never encountered xenobiotic compounds consisting of unusual structures/bonds or substitutions (Cl, NO₂, SO₃H, Br, CN, or CF₃). Therefore, they are unable to utilize them as substrate (in enzymatic degradation) which makes them recalcitrant in nature. Since last 5 decades, xenobiotic pollution has increased tremendously all over the globe. Over the years, through frequent exposures, various microorganisms have adapted to degrade some of the xenobiotics by producing novel enzymes which includes monooxygenases, dioxygenases, reductases, laccases, dehalogenase, organophosphate hydrolases, etc. (refer Fig. 1.1A). Microbial remediation of xenobiotics (refer Fig. 1.1B) is environmentally safe and economical but the rate of degradation/removal is very slow (slow kinetics and lack of enzyme specificity), which makes xenobiotic pollution persistent in nature and leads to environmental degradation.

In recent years, Advanced Oxidation Processes (AOPs) are gaining more attention due to their efficient degradation potential. An AOP is broadly defined as a set of redox reactions wherein the reactive intermediates produced such as $\cdot\text{OH}$, $\cdot\text{O}_2^-$, $\text{HO}_2\cdot$ carry out the oxidation of recalcitrant organic pollutants. The most commonly used AOPs

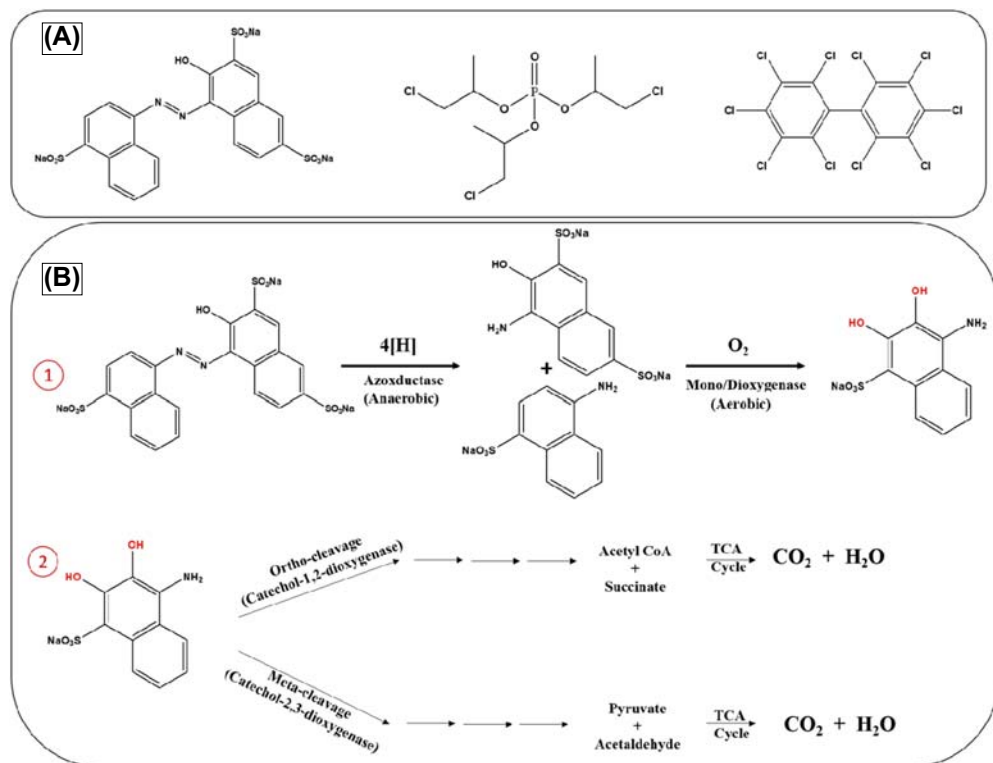


Figure 1.1 (A) Chemical structure of Amaranth dye, Tri(chloro-propyl) phosphate (TCPP), and PCB-209 (left to right). (B) Mechanism of microbial enzymatic decolourization and degradation of Amaranth dye.

include ozonation, Fenton reactions, electrochemical oxidation and heterogeneous photocatalysis using semiconductor catalysts. In comparison to the conventional physical, biological, and chemical treatments, AOPs provide the advantages of rapid reaction rates, enhances removal of total organic carbon (TOC), elimination of harmful toxicants, among others. Among AOPs, photocatalysis using heterogeneous semiconductor nanocatalyst is gaining wide significance as a “green” and effective technique to solve the existing problems of world energy crisis and environmental pollution using solar energy. But recently technological advancements have proved that the intimate coupling of photocatalysis with bioremediation (ICPB) as better alternative. It is an extremely efficient and environmentally friendly method for the treatment of wastewater contaminated with xenobiotic. This innovative synergistic technology is capable of completely treating the xenobiotic contaminated wastewaters in an efficient manner as compared to biodegradation and photocatalysis individually. This chapter discusses the recent advances in bioremediation, photocatalysis, and ICPB strategies for xenobiotics such as dyes,

pesticides, and chlorinated organic compounds in more details along with the drawbacks and future outlook of each of the remediation methods in the following sections.

1.2 Xenobiotic remediation methods

1.2.1 Bioremediation of xenobiotics

Xenobiotic degrading enzymes are divided into three types, i.e., phase I, phase II, and transporter enzymes. Lipophilic xenobiotics are first acted by phase I enzymes, whose purpose is to make xenobiotics more polar (sparingly soluble). Phase II xenobiotic utilizing enzymes are conjugating enzymes and directly interact with xenobiotics but mostly interact with intermediates produced by phase I enzymes. Passive and active transport enzymes eliminate the more polar degradation products formed upon degradation by phase I enzymes [12].

1.2.1.1 Biodegradation of azo dyes

Textile industries release colored effluents containing azo dyes which are toxic to aquatic life and increase chemical oxygen demand (COD) and biological oxygen demand (BOD) of clean waters. Azo dyes contain chromophore ($-N=N-$) and are difficult to degrade by microbial treatment. Mainly two microbial enzymes, azo-reductases, and laccases play important role in the azo dye degradation process [13]. Azo-reductase (EC1.7.1.1.6) degrades azo dyes by reducing it into colorless amines using FADH or NADH as electron donor. The azo-reductase cleaves $-N=N-$ by transferring four electrons (2 electrons in each step) to azo dye which acts as an electron acceptor resulting in decolorization by forming a colorless solution. Degradation of azo dyes in anaerobic condition is more efficient than the aerobic environment, as azo-reductase is an oxygen-sensitive enzyme. Laccase (EC1.10.3.2) belongs to the multi copper oxidase family of enzymes and is capable of efficiently degrading a wide range of xenobiotics and aromatic substrates. Laccases catalyze the degradation of azo dyes nonspecifically by targeting phenolic group of the dye using a free radical mechanism that forms phenolic compounds generating fewer toxic aromatic amines [14]. Peroxidase enzymes such as lignin peroxidase and manganese peroxidase are also potential azo dye degrading microbial enzymes. Zahran et al. [15] investigated that *E. faecalis* and *E. avium* can remove Amaranth dye 98.87% and 96.97% at aerobic and microaerophilic conditions by producing FMN-dependent-NADH azo-reductase. Similarly, Suwannawong et al. [16] reported 90% removal of Rhodamine B dye by *Latinos polychrous* capable of producing laccase enzyme. Furthermore, azo-reductase, NADH-DCIP reductase, and laccase producing microbial consortia (*E. coli* ENSD101, *E. ludwigii* ENSH201, and *B. thuringiensis* ENSW401) can remove 99% methyl orange [17].

1.2.1.2 Biodegradation of pesticides

Organophosphate (OP) pesticides are phosphate esters of alcohols and phosphoric acid with the general structural unit of $O=P(OR)_3$ [18]. OP is applied in agriculture as pesticides. OP toxicity is caused by the irreversible binding of OP compounds to acetylcholinesterase, found within the neuromuscular junction and thus inactivating it [18]. Organophosphate hydrolases (opdH) are enzymes produced by microorganisms to detoxify organophosphate pesticides. Di isopropyl fluorophosphatase (DFPase) or organophosphorus acid anhydrolase are identified as the potential OP degrading enzymes with enzyme code (EC:3.1.8.2), studied from microorganisms, *Loligo vulgaris* and *Alteromonas* sp. JD6.5, respectively [19]. Organophosphate pesticides called chlorpyrifos are degraded by the organophosphate hydrolyases (opdH) through novel intermediate 2,6-dihydroxypyridine by *Arthrobacter* sp. HM01 which was confirmed by TLC/HPLC/LCMS analysis [20]. WHO has declared carbamate (Carbaryl, Aldicarb, Methomyl, Carbofuran, and Propoxur) pesticides used to control many insects and pests of crops, as toxic, hazardous, and persistent in nature. Metabolic degradation of pesticide carbamates is catalyzed by carboxyl ester hydrolases (EC 3.1.1) which are known to catalyze the hydrolysis of carboxyl esters (EC 3.1.1), thioesters (EC 3.1.2), phosphoric (EC 3.1.4/5/7/8), and sulfuric (EC 3.1.6) esters. Enzymes Carboxylesterases are reported in various bacteria which includes *Blastobacter*, *Arthrobacter*, *Pseudomonas*, *Achromobacter*, and *Micrococcus* genera [21]. *Enterobacter* sp. stain BRC05 effectively degraded 79.77% of Carbofuran (Carbamate) by producing Carboxylesterases [22]. Ambreen et al. [23] investigated *Bacillus thuringiensis* MB497 producing Organo-phosphorous phosphatases capable of removing 81%–94.6% chlorpyrifos, Triazophos, and Dimethoate from contaminated site. Similar studies have been reported on PCBs which are presented in the next section.

1.2.1.3 Biodegradation of chlorinated organic compounds

PCBs are highly stable and toxic due to the presence of chlorine substituents and aromatic rings. The primary step in microbial degradation of PCB is dehalogenation (i.e., removal of the chlorine group) which is catalyzed by dehalogenase type of enzymes. During this process the chlorine substituent is replaced with hydrogen [24]. Reductive dehalogenation of halogenated aromatics is operational under anaerobic condition, whereas oxidative dehalogenation of PCBs by monooxygenases/dioxygenases takes place under aerobic conditions. Once chlorine atom is removed, further microbial degradation of PCB is via biphenyl dioxygenase enzyme (encoded by gene *BphA*) which results in deoxygenation of biphenyl to 2,3-dihydro-[1,1'-biphenyl]-2,3-diol. This is further acted upon by enzyme dihydrodiol dehydrogenase (encoded by gene *BphB*) which catalyzes dehydrogenation giving rise to intermediate [1,1'-biphenyl]-2,3-diol. Enzyme 2,3-dihydroxybiphenyl dioxygenase (*BphC*) cleaves aromatic ring of intermediate [1,1'-biphenyl]-2,3 diol through meta-cleavage pathway to 2-hydroxy-6-oxo-6-phenylhexa-2,4-dienoic acid (HOPDA). Furthermore, HOPDA hydrolytic degradation

is carried out by enzyme 2-hydroxy-6-oxo-6-phenylhexa-2,4-dienoate hydrolase (BphD) to benzoic acid and 2-hydroxy penta-2,4-dienoic acid [25]. Mono oxygenases and dioxygenases further degrade benzoic acid via ortho-cleavage or meta cleavage pathway and final degradation via TCA cycle. Benitez et al. [26] reported that *Pleurotus pulmonarius* LBM 105 capable of producing Lygnolytic enzymes can be applied to remove 95% PCBs from wastewater. Mixed culture of *Mycolicibacterium frederiksbergense* IN53, *Rhodococcus erythropolis* IN129, and *Rhodococcus* sp. IN306 when used for bioremediation of PCBs was found to reduce its original concentration to 51.8% by producing enzymes PphB and PphC [27]. Table 1.1 highlights the catalytic role of some of the significant enzymatic biocatalysts discussed above.

In spite of the several advantages discussed earlier, it is trivial that microbial bioremediation process is kinetically limited. Very few microbial enzymes can practically degrade the complex organic structures of the xenobiotics completely, thereby making them recalcitrant and persistent in nature. Most of these enzymes being selective in nature are unable to simultaneously degrade a mixture of xenobiotics in contaminated wastewaters. Therefore, there is a pressing need for an advanced, efficient, and environmentally friendly method for the effective treatment of xenobiotic contaminated wastewaters.

1.2.2 Advanced photocatalytic degradation of xenobiotics

Photocatalysis is the prominent type of AOP [2]. In general, the photocatalytic mechanism involves (i) adsorption of reactant on the surface of a semiconductor photocatalyst, (ii) generation of charge carriers and reactive oxygen species on the photocatalyst surface; (iii) catalytic reaction followed by (iv) the desorption of the products from the catalyst surface [7]. The photocatalytic oxidation of the xenobiotics typically proceeds in the presence of an energetic light source, a powerful oxidant (air or O₂) and an effective semiconductor photocatalyst [31]. Fig. 1.2A shows the image of a typical photocatalytic reactor used for treatment of xenobiotics. Photocatalysis was first used by German chemist Dr. Alexander Eibner in 1911 wherein he studied the bleaching of dark blue pigment of Prussian Blue using ZnO [32]. However, the real breakthrough in photocatalysis occurred in 1972 when photolysis of water was successfully carried out using TiO₂ photocatalyst [33], which has led to intense research using photocatalysis for various applications such as organic pollutant degradation, hydrogen production, CO₂ conversion, among others.

1.2.2.1 Photocatalysts

An effective photocatalyst must produce sufficient number of active charge carriers by harnessing maximum photons from the illumination source [34]. Semiconductors are an important class of solid crystalline materials in this regard, with their electrical conductivity and band gap energies lying between that of insulators and conductors. The moderate band gap values of semiconductors (1–4 eV) are suitable for various charge-transfer

Table 1.1 Literature reports on xenobiotics bioremediation strategies.

Xenobiotic	Contaminant	Microorganisms degrading	Enzymes studied	Reaction time	Initial concentration	% Degradation
Azo dyes	Amaranth dye	<i>E. faecalis</i> and <i>E. avium</i> [15]	FMN-dependent-NADH azoreductase	26 h	20×10^{-6} M	98.87%
	Rhodamine B	<i>Latinos polychrous</i> [16]	Laccase	52 h	10×10^{-6} M	90
	Methyl orange	<i>Consortia</i> (<i>E. coli</i> ENSD101, <i>E. ludwigii</i> ENSH201, and <i>B. thuringiensis</i> ENSW401) [17]	Azoreductase, NADH-DCIP reductase and laccase	60 h	200 ppm	99.29
Pesticides	Chlorpyrifos	<i>Bacillus cereus</i> Ct3 [28]	—	8 days	125 ppm	88
	Carbofuran (Carbamate)	<i>Enterobacter</i> sp. stain BRC05 [22]	Carboxyesterases	38 h	100 ppm	79.77
	Methyl parathion	<i>Bacillus pumilus</i> W1 [29]	Phosphotriesterase	24 h	250 ppm	70
Chlorinated compounds	Chlorpyrifos, Triazophos, and Dimethoate	<i>Bacillus thuringiensis</i> MB497 [23]	Organophosphorous phosphatases	30 min	50 ppm	81–94.6
	Polychlorinated biphenyl	<i>Penicillium chrysogenum</i> , <i>P. citreosulfuratum</i> , <i>P. canescens</i> , and <i>Aspergillus jensenii</i> [30]	Peroxidases, laccases, cytochrome P450 enzyme	5 days	1 ppm	70
	Polychlorinated biphenyl	<i>Mycolicibacterium frederiksbergense</i> IN53, <i>Rhodococcus erythropolis</i> IN129, and <i>Rhodococcus</i> sp. IN306 (mixed culture) [27]	PphB and PphC	6 months	—	84.5
	Polychlorinated biphenyl	<i>Pleurotus pulmonarius</i> LBM 105 [26]	Ligninolytic enzyme	24 h	85 ppm	95.4

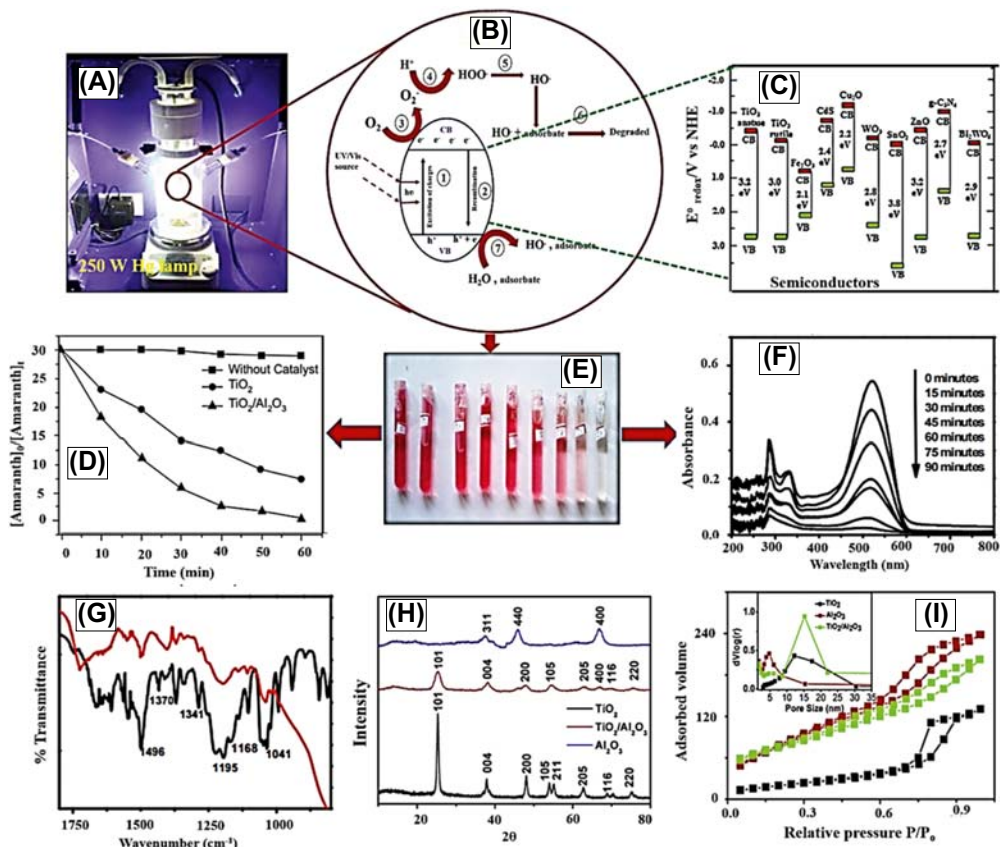


Figure 1.2 (A) Typical UV-Vis photochemical reactor. (B) Mechanism of photocatalytic degradation of xenobiotic over a semiconductor photocatalyst. (C) Band structure of different types of semiconductor catalysts. (D–F) Kinetic profiles of photodegradation of Amaranth dye over TiO_2 and $\text{TiO}_2/\text{Al}_2\text{O}_3$ monitored using UV-VIS spectrophotometer. (G) IR spectra of Amaranth dye (black) and adsorbed Amaranth dye on TiO_2 (red). (H) PXR overlay of TiO_2 , $\text{TiO}_2/\text{Al}_2\text{O}_3$ and Al_2O_3 . (I) N_2 -adsorption-desorption isotherm on TiO_2 , $\text{TiO}_2/\text{Al}_2\text{O}_3$ and Al_2O_3 catalysts used for Amaranth dye degradation. ((C) Reproduced with permission from M.K.H.M. Nazri, N. Sapawe, A short review on photocatalytic toward dye degradation, *Mater. Today Proc.* 31 (2020) A42–A47. <https://doi.org/10.1016/j.matpr.2020.10.967> Elsevier copyright, 2020; (D–F) Adapted with permission from P.P. Morajkar, A.P. Naik, S.T. Bugde, B.R. Naik, Chapter 20—photocatalytic and microbial degradation of Amaranth dye, in: S.N. Meena, M.M. Naik (Eds.), *Advances in Biological Science Research*, Academic Press, 2019, pp. 327–345. <https://doi.org/10.1016/B978-0-12-817497-5.00020-3> Elsevier copyright, 2019; (I) Adapted with permission from P.P. Morajkar, A.P. Naik, S.T. Bugde, B.R. Naik, Chapter 20—photocatalytic and microbial degradation of Amaranth dye, in: S.N. Meena, M.M. Naik (Eds.), *Advances in Biological Science Research*, Academic Press, 2019, pp. 327–345. <https://doi.org/10.1016/B978-0-12-817497-5.00020-3> Elsevier Copyright, 2019.)

processes such as photodegradation. An ideal photocatalyst should be highly active, must itself remain unaltered, and should get reproduced at the end of each catalytic cycle. The molecular orbitals of the solid semiconductor photocatalyst consists of a band structure. The band structure is broadly divided into two; the valence band (VB) and the conduction band (CB), which are separated by a moderate band gap (1–4 eV) [35] (see Fig. 1.2). For a semiconductor to be photochemically active as a catalyst, the reduction potential of the photogenerated electrons in the conduction band, must be sufficiently negative in order to reduce adsorbed oxygen to superoxide anion radical ($\cdot\text{O}_2^-$); while the oxidation potential of the photogenerated valence band holes must be sufficiently positive to generate $\cdot\text{OH}$ radicals [36]. Furthermore, for effective photon absorption, the energy of photons should be either higher or identical to the band gap energy of the semiconductor photocatalyst [7]. The process of photocatalysis starts with the illumination of the semiconductor photocatalyst's surface which induces charge separation between the valence band (VB) and the conduction band (CB) (refer Fig. 1.2B). Fig. 1.2C shows the band structure diagram of some of the commonly employed semiconductor photocatalysts.

The literature reports wide range of heterogeneous semiconductor catalysts which are being tried, tested, and improved for better photodegradation of toxic xenobiotics [2,7,9,37]. Among the commonly reported types of photocatalysts such as Metal—sulfides, nitrides, MOFs, oxides, phosphides, etc., metal oxides are gaining wider attention due to their higher photostability and reusability over several catalytic cycles. From the very beginning, TiO_2 is widely studied for photodegradation processes, due to its nontoxicity, chemical steadiness, and easy obtainability [2,7]. TiO_2 has emerged as a versatile semiconductor photocatalyst for the degradation of almost all types of xenobiotics including toxic dyes [2,31,38–40], pesticides [6,7], PCBs [9,11] etc. ZnO is another extensively studied photocatalyst for degradation of xenobiotics, due to its chemical stability, low cost, and wider light absorption spectrum than TiO_2 [41]. However, the wider band gap and rapid rates of recombination of photogenerated electron—hole pairs limits their photocatalytic activity. Researchers have tried to overcome this limitation by incorporating plasmonic materials like Ag on semiconductor materials such as Ag/TiO_2 [42], $\text{TiO}_2/\text{ZnO}-\text{Ag}$ [41] and $\text{Ag}-\text{Cu}_2\text{O}$ [43]. The localized surface plasmon resonance in Ag has greatly contributed in reduction of electron hole pair recombination rates. It also broadens the visible light uptake capacity of the metal oxide and thus together it contributes in enhancing the photocatalytic performance. In addition to these, the two-dimensional nanostructures of MoS_2 have recently gained a considerable attention in various catalytic applications due to its unique chemical and physical characteristics. The low band gap of 1.2 eV makes MoS_2 applicable in various field of catalytic application such as photocatalysis [44], hydrogen production [45] and dye-sensitized solar cells [46]. Additionally, it is also known as an excellent co-catalyst in synthesizing 2D heterojunction photocatalyst. Likewise, there are various single layered (ZrO_2 , ZnS , SnO_2 ,

NiO, CuO, Cu₂O, CdS, SiC, etc.) and multilayered (WO₃/NiWO₄, SnO₂/g-C₃N₄, ZnO@TiO₂, CuFeO₂/ZnO, etc.) photocatalysts which are reported in the recent literature [2,7,9]. The two or more components in case of multilayered photocatalysts, level out each others' limitations leading to better charge separation, low rates of charge-carrier recombination, and increased levels of visible light absorption. Thus, the multilayered photocatalysts with multiple valence and conduction bands are found to exhibit better photocatalytic activities compared to single layered photocatalysts.

1.2.2.3 Synthesis and characterization of semiconductor photocatalysts

Among all the synthetic methodologies employed for the synthesis of various single and double layered photocatalysts, hydrothermal, sol-gel, and chemical vapor deposition methods are the most popular. Hydrothermal method helps in the fabrication of morphologically tuned nanocatalysts [47]. Certain morphologies tend to expose large number of catalytic active sites which enhance the rate of photodegradation. Various morphologies such as nanoparticles [47], nanosheets [48], nanorods [49], etc., can be synthesized via adjusting reaction parameters such as temperature, time, solvent, and SDA (structure directing agents). For instance, TiO₂ prepared via sol-gel method was found to be highly porous (mesoporous) which showed very high activity for degradation of Amaranth dye [40]. The synthesized photocatalysts were characterized using FTIR (Fourier Transform Infrared Spectroscopy), HR-TEM (High resolution Transmission Electron Microscopy), SAED (Selected Area Electron Diffraction), PXRD (Powder X-ray Diffraction), and analysis techniques while its photocatalytic properties were studied using UV-DRS (Ultraviolet-Diffuse Reflectance Spectroscopy), PL (Photoluminescence), and BET (Brauner-Emmett-Teller surface area analysis) studies. Results of some of these techniques is presented in (refer Fig. 1.2G-I). Similar studies have also been reported for the synthesis and characterization of several double-layered photocatalysts.

1.2.2.4 Photocatalytic mechanism and surface kinetics

In heterogeneous photocatalysis a solid semiconductor interacts with the contents of the liquid phase. The first step in the photocatalysis process includes the transport of contaminants from liquid phase to the photocatalyst surface. Depending upon the acidic or basic nature of the organic contaminant, it attaches to the appropriate active sites on the surface of the photocatalyst. This is followed by photoreaction wherein various oxidation-reduction reactions occur on the surface of the catalyst. The photoreaction starts upon illumination of the photocatalyst's surface with a light source (UV or Visible) wherein the electrons (e⁻) in the VB are excited to the CB leaving behind positively charged holes (h⁺). The photogenerated electron-hole pairs facilitate all the redox reactions (refer Fig. 1.2).

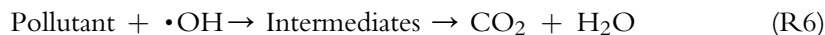
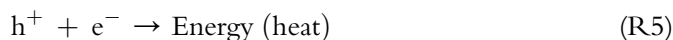
The holes generated in the VB carry out oxidation of either organic pollutant or water as depicted by the steps below,



The excited electrons in the CB reduces the adsorbed O_2 on the surface of the photocatalyst as shown below.



The detailed mechanism and reactions responsible for the photocatalytic degradation of an organic pollutant/contaminant can be summarized as follows:



Here, the $\cdot\text{OH}$ radical generated is the primary oxidizing agent while the adsorbed O_2 prevents the electron–hole pair recombination. In the absence of adsorbed O_2 , electrons accumulate in the CB and increase the rate of recombination of hole and electron pair [31]. Hence, it is important to prevent accumulation of electronic charge to overcome charge recombination which is one of the prominent limiting factors affecting effective photocatalytic process [7].

The highly reactive species such as electrons, holes, $\cdot\text{OH}$, and $\cdot\text{O}_2^-$ are capable of indiscriminately degrading all types of organic matter. These active ionic and radical species attack the resonating double bonds in an aromatic compound and facilitate ring opening as well as chain breakage in an organic compound thereby, converting it into an easily biodegradable intermediate products [50].

In general, the rate of photocatalytic degradation of organic contaminants/pollutants/xenobiotics can be well explained using the Langmuir–Hinshelwood kinetics model or pseudo–first-order kinetics model [5,51].

$$r = \frac{-dc}{dt} = \frac{kKC}{1 + KC} \quad (\text{E1})$$

wherein r is the rate of the reactant.

C is the concentration of pollutant at some time t

k represents the pseudo–first-order rate constant.

K represents the adsorption coefficient of the reactant.

At low initial concentration C_0 of the reactant, the above equation is simplified to a pseudo-first-order equation. Eqs. (E2) and (E3) represent the logarithmic and exponential forms of rate equations as below.

$$\ln (C_0 / C) = k \cdot t \quad (\text{E2})$$

$$C = C_0 e^{-k \cdot t} \quad (\text{E3})$$

The rate constant value (k) could be obtained from the plot of $\ln(C_0/C)$ versus time in the form of slope (refer Fig. 1.2D). Further, the half-life of the pseudo-first-order reaction can be calculated according to the equation.

$$t_{1/2} = \ln 2/k \quad (\text{E4})$$

1.2.2.5 Photocatalytic degradation of azo dyes

Azo dyes are classified into two types depending on their charge: cationic and anionic azo dyes. Amaranth [39] and Rhodamine B [52] are cationic azo dyes, while Methyl orange [53] is an anionic azo dye. The uncontrolled emissions of artificially synthesized azo dyes such as Acid Red 27 and Food Red 9 with complex aromatic structures, photostability, and low biodegradability has led to their accumulation in the environment, thereby leading to various health problems as discussed in the above section [39]. Several single layered and multilayered heterogeneous photocatalysts have been synthesized and utilized for degradation of azo dyes over the last few decades. The photocatalytic efficiencies of some of the most effective catalysts are listed in Table 1.2. So far, TiO_2 and ZnO are the most widely employed photocatalysts for the degradation of dyes [39,86]. However, the major limitation in case of these photocatalysts is their inherent recombination of charge carriers which in turn affects the formation of reactive intermediates or in situ oxidizing species such as $\cdot\text{OH}$ and $\cdot\text{O}_2^-$ radicals on the surface of the photocatalyst [2]. Also, the wider band gap (~ 3.2 eV (TiO_2) and ~ 3.4 eV (ZnO)) restricts their absorption capacity to narrow UV region and the visible region cannot be utilized for the generation of charge carriers. Moreover, as the nanoparticles naturally have the inherent property to agglomerate, large-scale synthesis of a high surface area ZnO and TiO_2 is still limited [39]. Nowadays, a lot of effort is being channelized to fabricate nanosized/porous TiO_2 and ZnO catalysts in order to increase its surface area and expose higher number of catalytic active sites [54,87]. Super porous TiO_2 fabricated by Naik et al. [54] showed better degradation efficiency of 95.6% than the nonporous TiO_2 (82.6%) for Amaranth degradation under similar photodegradation conditions, in lesser time duration [40] (refer Table 1.2).

Doping of parent photocatalyst with other transition metals is another method which is being investigated in several reports in order to improve the number of charge carriers and overcome the undesirable process of their recombination. Pascariu et al. [57] showed

Table 1.2 Literature reports on photocatalytic degradation of azo dyes.

Contaminant	Photocatalyst	Initial dye concentration	Light source	Reaction time	% Degradation
Amaranth dye	TiO ₂ [40]	30 ppm	250 W medium pressure Hg lamp	1.5 h	82.6
	Super porous TiO ₂ [54]	30 ppm	250 W Hg medium pressure lamp	15 min	95.6
	Fibrous Ni _{1-x} O nano-sponge [55]	30 ppm	250 W Hg medium pressure lamp	70 min	93.8
	YVO ₄ nano-powder [56]	1.04 × 10 ⁻⁵ M (5 ppm)	Natural sunlight of 0.767 kW/cm ² avg. light intensity	2 h	80
	ZnO:Ag [57]	10 ppm	100 W tungsten lamp	10 h	98.40
	Co _{0.25} Zn _{0.75} Fe ₂ O ₄ [58]	25 ppm	16 UV lamps (300 nm)	2 h	90
	N-doped WO ₃ [59]	5 ppm	160 W metal halide lamp	2 h	100
	Ag@RGO/g-C ₃ N ₄ [60]	5 × 10 ⁻⁵ M	15 W Sylvania UV-A lamp	2 h	81
	Rare earth doped YVO ₄ [61]	1 × 10 ⁻⁵ M	Sunlight	1 h	83
	TiO ₂ /Al ₂ O ₃ [39]	30 ppm	250 W Hg medium pressure lamp	1 h	98.6
	TiO ₂ /Pt-graphene oxide (GO) [62]	2 × 10 ⁻⁵ M	4 × 15 W UV light	3 h	99.56
	PAN/SiO ₂ -TiO ₂ -NH ₂ nanofiber [63]	10 ppm	125 W Xe lamp	30 min	95
BiVO ₃ /SnO ₂ [64]	5 × 10 ⁻⁵ M	300 W Xe lamp	1 h	92	

Continued

Table 1.2 Literature reports on photocatalytic degradation of azo dyes.—cont'd

Contaminant	Photocatalyst	Initial dye concentration	Light source	Reaction time	% Degradation
Methyl orange	ZnO microflowers [65]	10 ppm	9 W Hg lamp	5 h	90
	Bi ₂ O ₃ [66]	20 ppm	6 W UV-C lamps	2 h	93.76
	Floral ZnO [67]	10 ppm	UV light	30 min	92
	TiO ₂ /nanocellulose [68]	40 ppm	500 W UV lamp	30 min	99.72
	K ₂ Ti ₆ O ₁₃ nanorods [69]	10 ppm	300 W high pressure Hg lamp	1 h	—
	Ag—CdS@Pr-TiO ₂ core/shell NPs [70]	32 ppm	—	30 min	98
	Ti ₃ C ₂ —TiO ₂ [71]	30 ppm	Solar simulator	40 min	99
	Gd ₂ O ₃ -ZIF-8 [72]	0.0635 mM	UV light (254 nm)	40 min	98.05
	CeVO ₄ /BiVO ₄ @rGO [73]	10 ppm	250 W Xe discharge lamp	2 h	90
	Muscovite/W-TiO ₂ [74]	10 ppm	Simulator solar	2 h	98.4
	Ag/TiO ₂ /biochar [75]	20 ppm	500 W long arc Hg vapor lamp	1 h	97.48
	g-C ₃ N ₄ @ZnO/GO composites [76]	10 ppm	Simulated sunlight	2 h	92
	Co ₃ O ₄ —ZnO [77]	—	Sunlight	2 h	100
	Rhodamine B	TiO ₂ film [78]	15 ppm	5 W UV lamp	30 min
Au/ZnO [79]		10 ppm	60 W Hg lamp	3 h	95
BiFeO ₃ /g-C ₃ N ₄ [80]		40 ppm	Sunlight	40 min	96
ZnFe ₂ O ₄ @ZnO [81]		5 ppm	LED lamps	4 h	91.87
Zn@CdS [82]		0.5 mg/100 mL	Sunlight	135 min	93
Ag@g-C ₃ N ₄ /CoWO ₄ [83]		100 ppm	Sunlight	2 h	97
2D/2D TiO ₂ /g-C ₃ N ₄ [84]		10 ppm	500 W Hg lamp (UV)	2 h	99.9
Spindle-like Co ₃ O ₄ —ZnO [85]		10 ppm	125 W Hg lamp	1 h	98

that 1% Ag-doped ZnO showed higher photocatalytic activity (95.9%) than pristine ZnO (71.3%) for Amaranth dye degradation. Similarly, 95% photodegradation of Rhodamine B was achieved using Au/ZnO which was attributed to lowering of band gap of ZnO, upon addition of dopant [79]. Furthermore, agglomeration of nanoparticles can be avoided, by dispersing the active phase of TiO₂ and ZnO over support materials such as graphene oxide (GO) [88,89], xanthan gum [90], porous glass, Al₂O₃, SiO₂, and others. TiO₂–Al₂O₃ and TiO₂/Pt-Graphene Oxide (GO) showed 98.6% and 99.6% Amaranth dye degradation under 1 and 3 h irradiation using 250 W Hg Medium pressure lamp and 15 W UV-light source, respectively. While TiO₂/nanocellulose achieved 99.72% degradation of Methyl Orange in 30 min using 500 W UV lamp. Similar results were seen in case of other hybrid photocatalysts as depicted in Table 1.2. Fig. 1.2E and F shows gradual decolorization of Amaranth dye solution over TiO₂–Al₂O₃ catalyst [39]. The support materials, not only prevents the agglomeration of nanoparticles but also improves the adsorption of pollutant, which enhances its photocatalytic degradation. Next, various multilayered heterojunction photocatalysts have been developed by combining metal oxides with other photoactive materials, to overcome the problem of recombination of charge–carrier [39]. A heterojunction is the region of interface between two dissimilar semiconductors which helps to lower the band gap and prevent recombination of charge carriers due to the presence of multiple valence and conduction bands [2]. For instance, Co₃O₄–ZnO degraded 98% Rhodamine B using 125 W Hg lamp in 1 h and 100% Methyl Orange under sunlight irradiation in 2 h [77,85].

Apart from TiO₂ and ZnO, other metal oxides such as NiO [55], WO₃ [59], YVO₄ [56], etc., have been investigated for photocatalytic degradation of Amaranth dye. However, their degradation efficiency was below the desirable mark. Furthermore, heterojunction of these catalysts with other photoactive materials rendered better activities. The photodegradation efficiencies of various semiconductor catalysts for different dyes discussed above are listed in Table 1.2.

1.2.2.6 Photocatalytic degradation of pesticides

Although most of the pesticides are biodegradable in nature, they still persist in the environment for long time due to slow rates of biodegradation. Photocatalytic processes help to indiscriminately degrade wide range of pesticides, unlike the biological enzymes which are selective for a specific pollutant. According to the recent literature, very few photodegradation studies have been listed for the remediation of pesticides. Table 1.3 summarizes some of the recent reports on photodegradation of herbicides (Carbamates), insecticides (Organo-phosphorous compounds), and fungicides (Chloro-pyridines). Among others, organo-phosphorous insecticides such as chlorpyrifos, dimethoate, parathion, TCPP (Tri(chloro-propyl) phosphate), malathion, diazinon, etc., are the more commonly studied pesticides under photocatalytic conditions. In general, the photodegradation products of organo-phosphorous compounds include an inorganic moiety

Table 1.3 Literature reports on photocatalytic degradation of pesticides and chlorinated compounds.

Pesticide/chlorinated compounds	Contaminant	Photocatalyst	Initial dye concentration	Light source	Reaction time	% Degradation
Organo-phosphorous pesticides	Dimethoate	TiO ₂ [91]	0.05 M	250 W UV lamp	1 h	37.5
	TCCP	TiO ₂ nanosheets [92]	4 ppm	500 W Hg lamp	6 h	95
	Paraxon	Pd@ TiO ₂ nanoparticles [93]	31 ppm	570 W Xe lamp (OSRAM co)	2 h	86.6
	Diazinon	Ni@ZnO nanorods [94]	20 ppm	125 W medium pressure UVC lamp	2 h	86.44
	Malathion	Zn ⁺² @TiO ₂ nanoparticles [95]	177.59 ppm	125 W medium pressure Hg vapor lamp	81.04 min	98
	Parathion	ZnO/CuO [96]	20 ppm	400 W solar simulator lamp	1 h	100
	Dimethoate	ZnO/rGO [97]	5 ppm	250 W UV lamp	3 h	99
	Chlorpyrifos	CeO ₂ /TiO ₂ /SiO ₂ [98]	1–6 ppm	400 W UV lamp	1.3 h	81.1
	Chlorpyrifos	TCN/NiS (3D weed NiS) [99]	20 ppm	300 W Xe lamp	1 h	86
	Chlorpyrifos	mZnO/TiO ₂ -Fe ₃ O ₄ [100]	8 ppm	Visible light	50 min	94.8
	Chlorpyrifos	KIT-6/WS ₂ -Fe ₃ O ₄ (Korea Institute of Sci. and Tech.) [101]	7.2 ppm	—	52 min	92.1
	Chlorpyrifos	CuS-Bi ₂ O ₂ CO ₃ [102]	10 ppm	150 W Xe lamp	3 h	>95
	Imidacloprid	GO/Fe ₃ O ₄ /TiO ₂ -NiO [103]	10 ppm	300 W tungsten lamp	1 h	97.5
	Malathion	P3TA/Cu-TiO ₂ [104]	10 ppm	400 W high pressure Hg vapor lamp	2 h	100

Carbamate pesticides	Carbamate	Rare earth ion doped TiO ₂ [105]	20 ppm	300 W high pressure Hg lamp	3 h	>90
	Methomyl	ZnO [106]	16.2 ppm (1×10^{-4} M)	300 W Osram Ultra Vitalux lamp	1.5	93.5
	Thiobencarb	MoS ₂ [107]	5 ppm	Visible lamps (F4T5/CW Philips Lighting Co)	12 h	95
	Nitenpyram	Ag/Ag ₃ PO ₄ /Zn-Al LDH [108]	50 ppm	Visible light	1 h	100
Chloropyridines Chlorinated compounds	3-Chloropyridine	TiO ₂ [8]	40 ppm	150 W Xe lamp	3 h	100
	2-Chlorobiphenyl	TiO ₂ [51]	25 ppm	Simulated sunlight	1 h	90
	PCB-209	N-SiO ₂ [109]	7.93 ppm	500 W Xe lamp	4 h	98.5
	PCB 153	Fe ₃ O ₄ @SiO ₂ @TiO ₂ [110]	4 ppm	100 W UV LED	2 h	96.5
	Chlorinated biphenyls	Cu ₂ O-ACOF-1@Pd [111]	7×10^{-3} M	300 W Hg Xe lamp	1 h	95
PCB	CMCD-Fe ₃ O ₄ @TiO ₂ [112]	—	8 W UV lamp	16 min	83	

along with CO_2 and H_2O [92]. Like any other xenobiotic, TiO_2 and ZnO are the most commonly tested catalysts with efficiencies ranging from 30%–40%, 90%–95% to 99%–100% for OPs, Carbamates, and Chloro-pyridines, respectively [94].

Doping of TiO_2 with p-type impurity atom such as Zn introduces a greater number of holes. The excess holes create an acceptor level near the valence band of TiO_2 , which

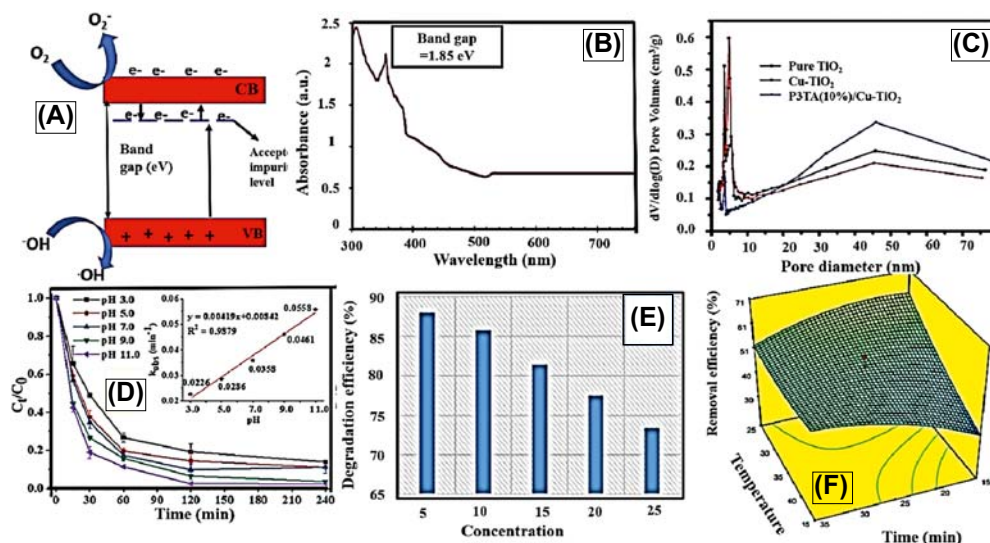


Figure 1.3 (A) Schematic showing charge transfer mechanism in doped photocatalyst. (B) UV-DRS spectrum of $\text{CeO}_2/\text{TiO}_2/\text{SiO}_2$ photocatalyst. (C) Comparative plot of pore volume v/s pore diameter of pure TiO_2 , Cu-TiO_2 , and P3TA@Cu-TiO_2 . (D) Effects of solution pH, on the photocatalytic degradation of PCB-209 over N-doped- SiO_2 -300 catalyst. (E) Effect of imidacloprid concentration on its photocatalytic degradation over $\text{GO}/\text{Fe}_3\text{O}_4/\text{TiO}_2\text{-NiO}$ catalyst. ((B) Reproduced with permission from R. Mansourian, S. Mousavi, S. Alizadeh, S. Sabbaghi, $\text{CeO}_2/\text{TiO}_2/\text{SiO}_2$ nanocatalyst for the photocatalytic and sonophotocatalytic degradation of chlorpyrifos, *Can. J. Chem. Eng.* (2021). <https://doi.org/10.1002/cjce.24157> Copyright 2021; (C) Reproduced with permission from I. Manga Raju, T. Siva Rao, K.V. Divya Lakshmi, M. Ravi Chandra, J. Swathi Padmaja, G. Divya, Poly 3-thenoic acid sensitized, copper doped anatase/brookite TiO_2 nanohybrids for enhanced photocatalytic degradation of an organophosphorus pesticide, *J. Environ. Chem. Eng.* 7 (4) (2019) 103211. <https://doi.org/10.1016/j.jece.2019.103211> Elsevier copyright 2019; (D) Reproduced with permission from C. Li, N. Wu, Y. Qi, J. Liu, X. Pan, J. Ge, et al., Preparation of nitrogen doped silica photocatalyst for enhanced photodegradation of polychlorinated biphenyls (PCB-209). *Chem. Eng. J.* 425 (2021) 131682. <https://doi.org/10.1016/J.CEJ.2021.131682> Elsevier, copyright 2021; (E) Reproduced with permission from F. Soltani-nezhad, A. Saljooqi, T. Shamspur, A. Mostafavi, Photocatalytic degradation of imidacloprid using $\text{GO}/\text{Fe}_3\text{O}_4/\text{TiO}_2\text{-NiO}$ under visible radiation: optimization by response level method. *Polyhedron* 165 (2019) 188–196. <https://doi.org/10.1016/j.poly.2019.02.012> Elsevier, Copyright 2019. (F) Effect of temperature and time on photocatalytic degradation of PCB-4 Reproduced with permission from S. Khammar, N. Bahramifar, H. Younesi, Preparation and surface engineering of $\text{CM-}\beta\text{-CD}$ functionalized $\text{Fe}_3\text{O}_4@\text{TiO}_2$ nanoparticles for photocatalytic degradation of polychlorinated biphenyls (PCBs) from transformer oil. *J. Hazard Mater.* 394 (2020) 122422. <https://doi.org/10.1016/j.jhazmat.2020.122422> Elsevier, Copyright 2020.)

facilitates easy electron injection and enhances charge collection leading to better charge separation (refer Fig. 1.3A) [95]. Similarly, ZnO is mainly doped with atoms of Ni, Cu, Ga, Sn, In, Al, Y, and Sc. Ni-doped ZnO nanorods were found to exhibit 99.97% conversion of diazinon pesticide under photocatalytic conditions [94]. Furthermore, formation of Z-scheme heterojunctions provides high redox stability and suppress recombination of photogenerated charges. TiO₂ and ZnO combined with other materials such as GO (graphene oxide), Silica, other oxides, and polymers are found to display enhanced photocatalytic degradation efficiency for organo-phosphorous compounds [96–98,100,103,104]. This can be attributed to decrease in band gap energy and improved charge separation (refer Fig. 1.3B). Moreover, materials such as GO contain abundant oxygen-containing groups on its surface which enable it to combine with many inorganic materials through covalent and/or ionic bonding to form composite catalysts [97]. Polymer materials such as polythiophene, poly-pyrrole, P3TA (Poly 3-Theonic acid), etc., help in surface sensitization of metal oxide catalysts owing to their high visible light absorption capacity, greater stability, and high mobility of charge carriers [104]. The composite of P3TA@Cu–TiO₂ was found to show enhanced surface area and pore volume as compared to pure TiO₂ (refer Fig. 1.3C)

Recently, nanostructured semiconductor sulfides such as WS₂, NiS, CuS, etc., have shown better photocatalytic potential than single oxides such as TiO₂. However, its lack of photostability is a major disadvantage. Hence, composites of metal sulfides with other metal oxides are found to be excellent photocatalysts for degradation of organo-phosphorous pesticides [99,101,102]. Photocatalytic degradation of carbamate pesticides is a more tedious process as compared to organo-phosphorous insecticides owing to their rigid organic structures. The photocatalytic efficiencies of various single and multi-layered catalysts for various Carbamate pesticides are also listed in Table 1.3 [105,108]. Only a limited literature on the photocatalytic degradation on chloro-pyridines and its derivatives leading to its complete mineralization under both UV light and sunlight is available [8]. Furthermore, the toxicity analysis revealed that the intermediate products formed to be more toxic as compared to the pollutant and required further monitoring. Hence, there is wide scope for development of more efficient photocatalysts and degradation processes which can mineralize wide spectrum of pesticides into environmentally benign products.

1.2.2.6 Photocatalytic degradation of chlorinated organic compounds

Unlike any other xenobiotics discussed so far, complete degradation of chlorinated organics in particular PCBs using biological processes is almost impossible or may take years. Most of the biological enzymes are unable to catalyze dehalogenation of multiple chlorine atoms. Photocatalytic degradation of these persistent organic chemicals is highly promising and depends mainly on its structure, nature of solvent, catalyst, and presence of oxidants [9]. PCBs are insoluble in water, hence most of the photocatalytic studies are

carried out in organic solvents. In general, the reactivity's of chlorine atoms at various positions of PCB rings are in the order: ortho > meta > para. Hence, the light-induced degradation of planar PCBs with no chlorine atom at ortho position is much slower as compared to perpendicular PCBs with ortho-Chlorine atom [51]. The research on photocatalytic degradation of PCBs is progressing rapidly in last few decades. Some of the recently reported catalysts and their photodegradation efficiencies are listed in Table 1.3 [109–112]. The photocatalytic degradation efficiency of TiO_2 for removal of PCBs was tested by Huang et al. in one of the earliest studies and achieved 90% removal of 2-Chlorobiphenyl in 1 h under natural sunlight. Furthermore, like before doped and multilayered heterojunction photocatalysts were found to exhibit higher degradation efficiency than single-layered photocatalysts. N-doped SiO_2 achieved 98.5% degradation of PCB-209 in 4 h using 500 W Xe lamp. 95% and 96.5% PCBs were removed using heterojunction catalysts such as $\text{Cu}_2\text{O-ACOF-1@Pd}$ and $\text{Fe}_3\text{O}_4@\text{SiO}_2@\text{TiO}_2$, respectively, under various light and reaction conditions as mentioned in Table 1.3 below. However, the photocatalytic degradation process in general produces intermediates which are more toxic than the xenobiotic itself, hence further mineralization of these toxic intermediates is absolutely essential. In recent years this can be efficiently carried out by intimately coupling photocatalytic degradation process with biodegradation, which will be discussed in detail in the following section.

1.2.3 Intimate coupling of photocatalysis with biodegradation methods

ICPB is an advanced and innovative method that combines AOPs with bioremediation strategies for efficient treatment of xenobiotic contaminated wastewater. Here, AOP such as photocatalytic degradation technology will initially degrade the recalcitrant xenobiotic compound into structurally simpler intermediate products which can be easily biodegraded by the microorganisms. In general, ICPB degradation is of two types: sequential and simultaneous. In sequential processes, the photocatalytic degradation of xenobiotics is followed by microbial degradation or vice-versa [50] (refer Fig. 1.4A). These processes are quite effective for degradation of organic contaminants/xenobiotics but are tedious and time consuming. Furthermore, the photocatalytic processes may generate toxic radicals by overoxidizing the organic compounds [113]. Hence, it becomes essential to restrict the sequential integrated process before the organic compounds overoxidize. In order to address this issue, researchers have come up with the idea of simultaneous ICPB degradation wherein there is simultaneous photobiodegradation taking place in a single reactor with the help of nano-enzyme type of catalysts. This technique has helped to overcome the uncertainties in sequential photocatalytic-biodegradation in terms of the type of intermediates formed. ICPB is also found to increase mineralization efficiency and lower the costs of operation [114]. Fig. 1.4B depicts the typical ICPB mechanism taking place in an ICPB reactor.

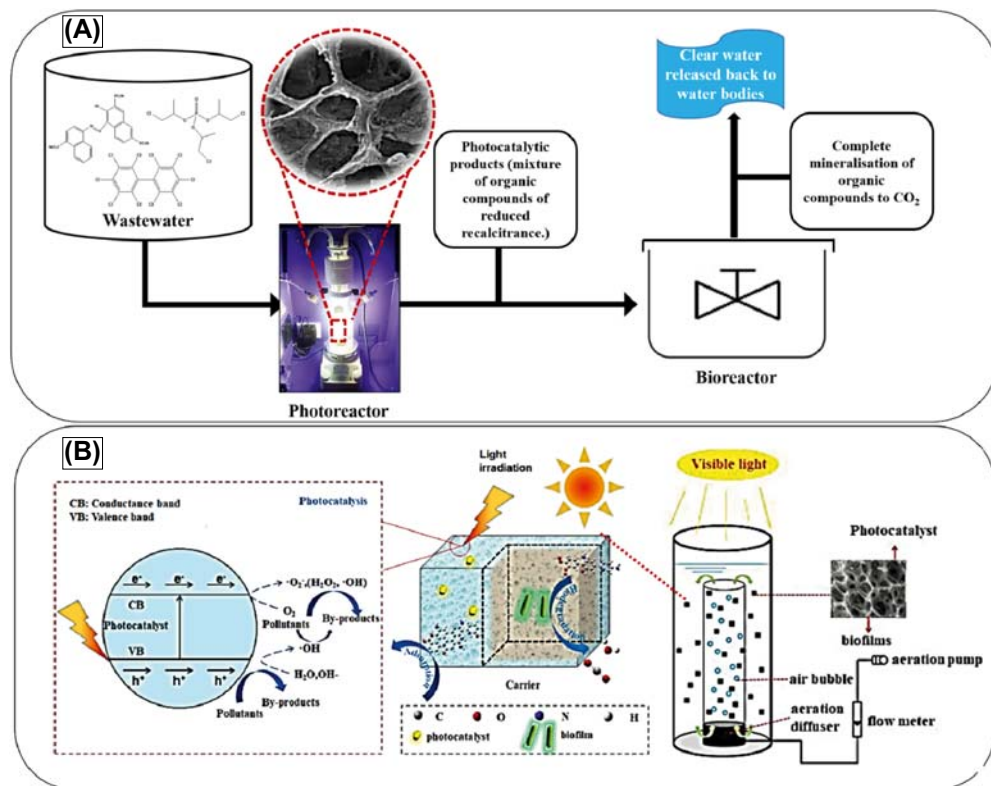


Figure 1.4 (A) Schematic of sequential photocatalytic and biological treatment of wastewaters containing xenobiotics. (B) Schematic of a typical ICPB reactor along with the mechanism of photobiodegradation process. ((A) SEM image reproduced with permission from S. Shoabargh, A. Karimi, G. Dehghan, A. Khataee, A hybrid photocatalytic and enzymatic process using glucose oxidase immobilized on TiO₂/polyurethane for removal of a dye, *J. Ind. Eng. Chem.* 20 (5) (2014) 3150–3156. <https://doi.org/10.1016/J.JIEC.2013.11.058> Elsevier copyright 2014; (B) Reproduced with permission from M. Yu, J. Wang, L. Tang, C. Feng, H. Liu, H. Zhang, et al., Intimate coupling of photocatalysis and biodegradation for wastewater treatment: mechanisms, recent advances and environmental applications, *Water Res.* 175 (2020) 115673. <https://doi.org/10.1016/J.WATRES.2020.115673> Elsevier, Copyright 2020.)

1.2.3.1 ICPB mechanism

The mechanism of ICPB involves (1) adsorption of the xenobiotics by the porous carrier, which in turn enhances its mass transfer to the surface of the photocatalyst. The photocatalyst's surface consists of various reactive oxidative species (ROS) which facilitate the photodegradation of xenobiotic. (2) The photocatalytic degradation involves absorption of photon energy ($h\nu$) wherein $h\nu >$ band gap energy excites the electrons from VB to CB, thereby generating electron–hole pairs. Simultaneously, the xenobiotic undergoes degradation via attack by the ROS and the holes. (3) The photoelectrons generated are transferred to the biofilm through c-type cytochromes, wherein the products of

photocatalysis are completely mineralized into CO_2 and water (biodegradation) [50,113]. The regular biodegradation of products of photocatalysis prevents damage to microbial metabolism and avoids unwanted oxidation. The simultaneous processes in ICPB are further augmented by the synergistic effect, wherein the photocatalysis and biodegradation are interdependent on each other. It is seen that the shear forces and generated free radicals can cause detachment of the biofilm from the carrier surface and lead to gradual decrease in biodegradation with the continuous enhancement of photocatalytic process. While the amount of photo catalytically degraded products increases to certain degrees, the organics in solution may conductively cause the formation of biofilms which enhances the biodegradation process. This balancing effect is called the Synergistic effect in ICPB mechanism [50].

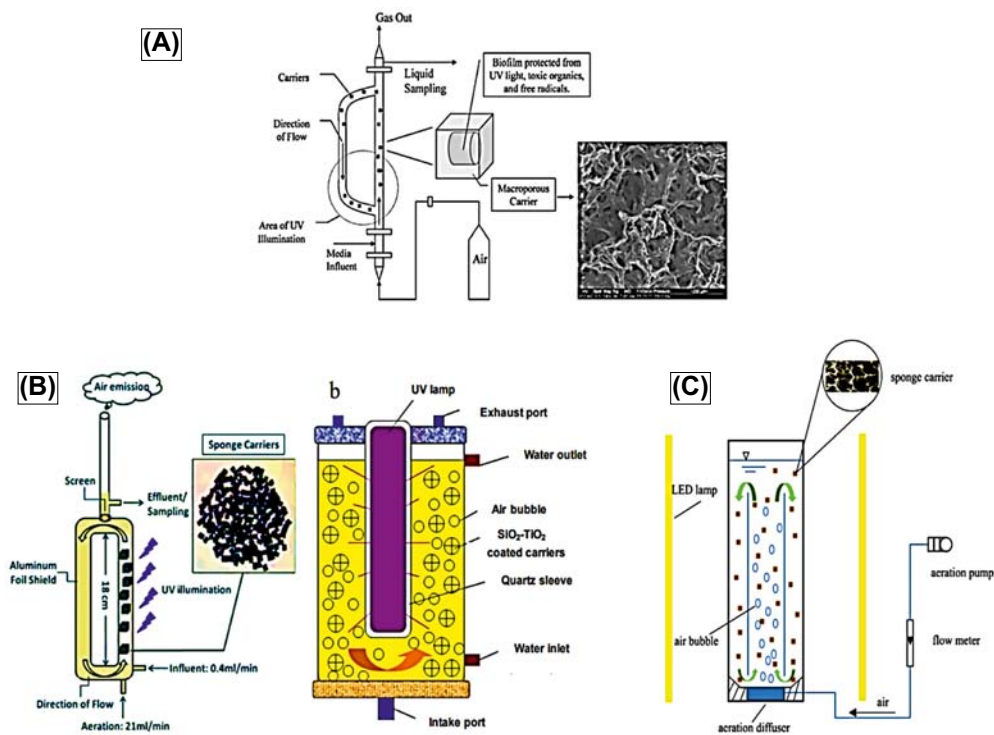


Figure 1.5 (A) Schematic of a PCBBR system utilizing macroporous cellulosic carrier along with FESEM image of photocatalyst. Schematic of (B) UPCBBR system (C) VPCBBR system. (Reproduced with permission from M. Yu, J. Wang, L. Tang, C. Feng, H. Liu, H. Zhang, et al., *Intimate coupling of photocatalysis and biodegradation for wastewater treatment: mechanisms, recent advances and environmental applications*, *Water Res.* 175 (2020) 115673. <https://doi.org/10.1016/J.WATRES.2020.115673> Elsevier, Copyright 2020.)

1.2.3.2 Photocatalytic circulating-bed biofilm reactor

The amalgamate of photocatalysis and biodegradation to treat wastewater can be performed in a bioreactor/photocatalytic circulating-bed biofilm reactor (PCBBR) (Fig. 1.5A). Depending upon the light source used, there are two types of PCBBR, i.e., visible light-driven photocatalytic circulating-bed biofilm reactor (VPCBBR) and UV light-driven photocatalytic circulating-bed biofilm reactor (UPCBBR) [115]. Fig. 1.5B and C show models of VPCBBR and UPCBBR, respectively. This bioreactor to treat wastewater using the above discussed synergistic technology should be designed in such a way that bacteria degrading products of photocatalysis should be protected from UV light and toxic oxygen reactive species. Macroporous cellulosic cubes are used in this technology that act as macroporous carriers made up of poly-urethane (PU) to protect the biofilm from UV radiations. Microporous materials which can facilitate exchange of wastewater and gases but trap xenobiotic degrading bacteria (biofilm). These bacteria are thereby protected by microporous materials from bactericidal UV radiations, free radicals, and toxic xenobiotics. Recently, visible light-driven ICPB processes are gaining importance and are found to exhibit better photocatalytic-biodegradation efficiencies than UPCBBR. For instance, Xiong et al. [116] used visible light-driven ICPB to evaluate the removal and mineralization of Tetracycline hydrochloride (TCH) with Ag/TiO₂ photocatalyst. TCH degradation was enhanced by ~23% over photocatalysis. Moreover, research on ICPB is still in its infancy and most of its aspects are still undiscovered. Additionally, this approach requires further technical developments to overcome difficulties such as loss of microbial biomass upon UV exposure and costly microporous carriers are required to protect the microbes from the effect of UV light.

1.2.3.3 Recent developments in mitigation of xenobiotics using ICPB

Several recent reviews have summarized the ICPB degradation of various xenobiotics such as dyes, pesticides, nitrogenous compounds, phenolic compounds, antibiotics, and chlorinated compounds [113,115,117,118]. Table 1.4 presents some of these important literature reports on ICPB remediation of xenobiotics. The first report on ICPB was documented by Rittmann et al. [114] in the year 2008 wherein the PCBBR was used for degradation of 2,4,5-trichlorophenol (2,4,5-TCP). Individually, biodegradation and photocatalysis were not able to completely degrade 2,4,5-TCP while the ICPB treatment enhanced its degradation to a significant extent. In a similar study, Li et al. [125] tried to further improve the degradation of 2,4,5-TCP by replacing the cellulosic carriers by a new commercially available microporous sponge cube, that was resistant to charring by the UV irradiation and hydroxy radical attack, unlike cellulose. The 2,4,5-TCP removal improved to 98% from 23.6% in the previous study. Further, 100% ICPB degradation of 2,4,5-TCP was achieved by using ceramic biofilms [124]. In another study, mesoporous SiO₂-TiO₂/PUF carriers were also found to exhibit excellent ICPB degradation efficiency for 2,4,5-TCP as induction of SiO₂ on TiO₂ prevented phase

Table 1.4 Intimate coupling of photocatalysis and biodegradation.

Xenobiotic	Contaminant	Photocatalyst	Microorganisms	Initial concentration	Reaction time	% Degradation
Azo dyes	Rhodamine B [119]	Macro/mesoporous anatase TiO ₂	Ceramic	10 ppm	3 h	98.8
	Methylene blue [120]	TiO ₂	Activated sludge	5 ppm	6 h	92.08
	Black 5 (RB5) [121] azo dye	(UV/TiO ₂)	<i>Candida tropicalis</i> JKS2	200 ppm	2 h	94.8
	Acid orange 7 [122]	GO _x /TiO ₂ /PU	<i>Glucose oxidase</i>	20 ppm	22 min	>99
Pesticide	Imidacloprid [123]	TiO ₂	<i>Enterobacter</i> sp. strain <i>ATA1</i>	50 ppm	18 h	94.6
Chlorinated compounds	2,4,6-TCP [124]	Without catalyst	Biofilm (ceramic)	20 ppm	3 h	95
	2,4,5-TCP [114]	P25 TiO ₂	Biofilm (cellulose)	70 μM	290 h	23.6
	2,4,5-TCP [125]	TiO ₂	Biofilm (BioCAP)	50 μM	24 h	92
	4-Chlorophenol [126]	N-TiO ₂	Carbon foam	20 ppm	12 h	90.5
	Chlorinated products from bleaching contaminated wastewaters [127]	TiO ₂ /bagasse cellulose composite	<i>Phanerochaete</i>	28 ppm	12 h	~100
Antibiotics	Tetracycline hydrochloride [128]	BiOCl/Bi ₂ WO ₆ /Bi ternary composites	Activated sludge	30 ppm	10 h	97.2
	Beta-apyoxytetracycline [129]	Bi ₁₂ O ₁₇ C ₁₂	Microbes isolated from swine farm	10 ppm	4 h	96.1
	Tetracycline [116]	Ag-doped TiO ₂	Activated sludge	30 ppm	8 h	~85
	Tetracycline [130]	Nano-particulate Ag/TiO ₂	Activated sludge	30 ppm	10 h	95
	Tetracycline [131]	Ag/TiO ₂ nanoparticles	Activated sludge	30 ppm	8 h	94
	Amoxicillin [132]	Ag-doped TiO ₂	Activated sludge	20 ppm	8 h	55
	Cephalosporin [133]	Ag-decorated single-crystal black TiO ₂ nanosheets	Activated sludge	—	10 h	96.1

transformation in TiO_2 . This led to increased number of surface reactive sites along with improved photon utilization, microorganism loading and organic molecule adsorption [134]. Similar studies are reported for the degradation of 4-Chlorophenol [126,135] and chlorinated wastewaters via ICPB technology [127]. Within 12 h of irradiation, the photobiodegradation system was able to achieve complete removal of chlorinated by-products (refer Table 1.4).

Moreover, the application of ICPB to dyes, pesticides, and PCBs is still very limited but holds great potential for their effective degradation. In the early works of Shoabargh et al. [122] it is noted that they have managed to achieve very high efficiency of photobiodegradation of Acid Orange 7 (a derivative of Amaranth dye) with >99% efficiency using the $\text{GO}_x/\text{TiO}_2/\text{PU}$ and *Glucose oxidase*. Similarly, Xing et al. [119] achieved 98.8% Rhodamine B removal using an advanced macro/mesoporous anatase TiO_2 ceramic floating photocatalyst. In another study, Rittmann et al. [117] tried degradation of three reactive dyes, namely Reactive Black 5, Reactive Yellow 86, and Reactive Red 120 using the original method employed for 2,4,5-TCP degradation. Around 97% degradation of Reactive Black five was achieved. Furthermore, Li et al. [136] were able to achieve fivefold better degradation of Reactive Black five by improving the sintering method of the TiO_2 catalyst. Zhang et al. [118] investigated the photocatalytic-biodegradation of dye-contaminated wastewater using a novel composite of g- C_3N_4 -P25/photosynthetic bacteria and managed to achieve 94% degradation efficiency. Xiong et al. [120] devised another novel hybrid composite carrier, SBC (Sugarcane bagasse cellulose)- TiO_2 and tried degradation of Methylene blue (MB). The ICPB degradation of MB (92.08%) was found to be much better as compared to biodegradation (70.26%) and photocatalysis (83.29%) tried individually. Moreover, no reports were found on the ICPB degradation of pesticides. In one of the recent studies [123], a comparison is made between biodegradation, photocatalysis, and sequential photobiodegradation of imidacloprid (pesticide) using TiO_2 photocatalyst and *Enterobacter* sp. strain ATA1. Around 83% degradation of imidacloprid was achieved after 15 days via sequential processes. Hence, by employing ICPB processes, much higher degradation efficiency for pesticides such as imidacloprid can be achieved although longer reactions times is a limiting factor.

Antibiotics are another well-known class of xenobiotics. TCH and its derivatives are the most commonly studied antibiotics [116,130–132]. The polyaromatic ring structure of tetracycline is mainly responsible for its longer half-life in the environment [129]. Many research groups have tried to improve the ICPB degradation protocol of TCH by means of light source [116], co-substrate [130], improvement of the rate of loading the photocatalyst [129], reactor design [133], etc. Ma et al. [131] managed to develop a simplified kinetic model for predicting the removal efficiency and mineralization of TCH. The developed model was found to accurately predict the ICPB efficiencies and revealed the mechanism of ICPB. Furthermore, like any other xenobiotic, the antibiotic wastewater treatment products may have toxic effects on aquatic as well as

terrestrial organisms. Wang and the group carried out biotoxicity analysis of degradation products of amoxicillin and reported that the degradation products of ICPB ($C_7H_{14}N_2O_2S$ [M.W. = 190], $C_7H_{13}NO_2S$ [M.W. = 175], and $C_8H_8O_3$ [M.W. = 152]) were much simpler and harmless as compared to degradation products of biodegradation ($C_{16}H_{18}N_2O_4S$ [M.W. = 334], $C_{15}H_{21}N_3O_3$ [M.W. = 291], $C_{14}H_{21}N_3O_3S$ [M.W. = 311]), and photocatalysis ($C_{14}H_{21}N_3O_2S$ [M.W. = 295]) obtained individually [132]. In summary, ICPB was found to exhibit better degradation efficiency than the individual processes. Hence, ICPB holds immense scope as the sustainable, potential solution toward the treatment of wastewater contaminated with recalcitrant xenobiotics such as azo dyes, pesticides, and PCBs.

1.3 Challenges and future outlook

So far ICPB has proven its potential for xenobiotic degradation in terms of efficiency and its versatility. However, there are certain limitations and shortcomings of this technology which has to be addressed before crowning it to be the ideal xenobiotic remediation method. Although the degradation pathways and ICPB mechanism for pollutant degradation are well explored, it lacks an in-depth comprehensive understanding of the process in some of the following aspects: (A) The structure and properties of many of the intermediate products of ICPB are still unidentified and lack experimental evidence. Hence, the microbial mineralization mechanism of photocatalytically generated intermediates is still unknown. (B) Many studies have reported the toxic effects of photocatalytic intermediate products on microbes, but the underlying mechanisms are unknown along with the resistance adaptations of microorganisms. (C) The rate of electron transfer from photocatalyst to biofilm via c-type cytochrome is a crucial step in the ICPB mechanism that facilitates the microbial mineralization process of photocatalytic intermediate products. This needs to be further investigated to improve electron transfer efficiency.

The evaluation of cost, recyclability of carriers and photocatalysts, and environmental compatibility of ICPB is still a concern which may hinder the commercial applicability of the process. Most of the ICPB studies discussed so far have investigated degradation of a single contaminant that too in the laboratory conditions. On the contrary, the actual wastewater polluted sites contain multiple contaminants which may inhibit the microorganisms employed, thereby leading to dysfunctioning of the ICPB system. The photon source poses a major restriction on practicability of ICPB. The huge amount of energy contained in UV light due to their short wavelengths (100–400 nm) can be efficiently utilized in UV photocatalysis to convert photon energy into chemical energy. However, this energy is sufficient to destroy the biofilm on interior as well as exterior of the carrier. UV light has antimicrobial activity since it leads to mutation in microbial DNA and thus affects their replication process. The cellular proteins in the outer membrane of the cells absorb UV photons upon exposure to UV light which ultimately leads to membrane

disruption, leakage of protoplasm and cell death. In recent years, visible light—driven photocatalysis or VPCB has gained lot of attention as visible light is harmless to microorganisms. However, UV light accounts to approx. 4% of the entire spectrum, which also limits its utility in ICPB technology.

The following solutions to the above problems were proposed by Zou et al. [50] which needs further research and holds the key to effective utilization of ICPB for xenobiotic remediation: (1) Use of advanced spectroscopy, microbial metabolomics, and mass spectrometry can together help to reveal the degradation pathways and mechanisms which in turn will aid in the enhancement of the efficiency of the process as a whole. (2) The recently designed advanced models of photobiodegradation hybrid systems are capable of providing better insights into the electron transfer mechanism between the biofilm and the photocatalyst which may decode the mineralization mechanisms of photocatalytic intermediates. (3) Tools such as Microtox acute toxicity test can help in toxicity analysis of the intermediates in ICPB [137]. (4) It is essential to conduct analysis of wastewaters and identification of the existing contaminants before subjecting it to ICPB. (5) Improved reactor design and synthesis of novel and active nanoenzymes or a nanocatalyst and microbial enzyme hybrid system is extremely essential in improving both activity and stability of the hybrid catalyst. Hence, with persistent research in the above strategies, it is possible that ICPB may emerge as an ultimate solution for xenobiotic mitigation in the future.

1.4 Summary and conclusion

Xenobiotics such as dyes, pesticides, and chlorinated compounds are some of the major pollutants which are being discharged untreated into the water bodies, from various textile, paint, leather, and food industries. These re-calcitrant chemicals are prone to cause major damage to the aquatic systems as well as human health. Bioremediation using natural microbial enzymes is an eco-friendly pathway but it is an extremely slow process. Also, enzymes being selective in nature are unable to degrade mixture of xenobiotics. Moreover, most of the xenobiotics such as complex PCBs are resistant to microbial degradation. To overcome these challenges, AOPs such as photocatalysis using semiconductor catalyst has gained wide attention. Photocatalytic degradation of xenobiotic is found to occur at a much faster rate as compared to conventional biodegradation processes. However, photocatalysis generates toxic degradation intermediates which require further degradation, which is an energy intensive process and involves complicated processes which require tedious optimization. Designing of an effective visible light photocatalyst still remains as a challenge although several homogeneous and heterogeneous photocatalysts and their composites are reported. Z-Scheme heterojunction type of photocatalysts are seen to exhibit excellent photocatalytic performance as compared to single metal oxides. Hence, there is a wide scope to devise an effective heterojunction-based

semiconductor photocatalysts with enhanced charge separation and low rates of recombination to further enhance the rates of degradation of xenobiotics. Further advancement in this field have led to the development of intimately coupled photobiodegradation technology. Fabrication and usage of nano-enzyme catalyst is found to help overcome the problem of microbial deactivation under UV light. So far, ICPB has performed exceedingly better than photocatalysis and biodegradation processes, for the remediation of xenobiotics. ICPB has the potential to completely remove xenobiotics. It is a comparatively less time consuming and an eco-friendly process as it avoids the formation of toxic products. However, not many studies have been reported in the context of field implementation of ICPB and most studies are limited to laboratory scale. It therefore opens a new doorway of opportunities to try the effectiveness of ICPB technology for field applications in remediating large spectrum xenobiotics from wastewater.

References

- [1] R. Ameta, S. Benjamin, A. Ameta, S.C. Ameta, Photocatalytic degradation of organic pollutants: a review, *Mater. Sci. Forum* 734 (2013) 247–272, <https://doi.org/10.4028/www.scientific.net/MSF.734.247>.
- [2] H. Anwer, A. Mahmood, J. Lee, K.-H. Kim, J.-W. Park, A.C.K. Yip, Photocatalysts for degradation of dyes in industrial effluents: opportunities and challenges, *Nano Res.* 12 (5) (2019) 955–972, <https://doi.org/10.1007/s12274-019-2287-0>.
- [3] G.M. Ziarani, R. Moradi, N. Lashgari, H.G. Kruger, Chapter 4—azo dyes, in: G.M. Ziarani, R. Moradi, N. Lashgari, H.G. Kruger (Eds.), *Metal-Free Synthetic Organic Dyes*, Elsevier, 2018, pp. 47–93, <https://doi.org/10.1016/B978-0-12-815647-6.00004-2>.
- [4] D. Saini, R. Aggarwal, A.K. Sonker, S.K. Sonkar, Photodegradation of azo dyes in sunlight promoted by nitrogen–sulfur–phosphorus codoped carbon dots, *ACS Appl. Nano Mater.* 4 (9) (2021) 9303–9312, <https://doi.org/10.1021/acsnm.1c01810>.
- [5] D. Vaya, P.K. Surolia, Semiconductor based photocatalytic degradation of pesticides: an overview, *Environ. Technol. Innov.* 20 (2020) 101128, <https://doi.org/10.1016/j.eti.2020.101128>.
- [6] M. Hadei, A. Mesdaghinia, R. Nabizadeh, A. Mahvi, S. Rabbani, K. Naddafi, A comprehensive systematic review of photocatalytic degradation of pesticides using nano TiO₂, *Environ. Sci. Pollut. Control Ser.* 28 (2021), <https://doi.org/10.1007/s11356-021-12576-8>.
- [7] K. Bano, S. Kaushal, P.P. Singh, A review on photocatalytic degradation of hazardous pesticides using heterojunctions, *Polyhedron* 209 (2021) 115465, <https://doi.org/10.1016/j.poly.2021.115465>.
- [8] M.C. Ortega-Liébana, E. Sánchez-López, J. Hidalgo-Carrillo, A. Marinas, J.M. Marinas, F.J. Urbano, A comparative study of photocatalytic degradation of 3-chloropyridine under UV and solar light by homogeneous (photo-Fenton) and heterogeneous (TiO₂) photocatalysis, *Appl. Catal. B* 127 (2012) 316–322, <https://doi.org/10.1016/j.apcatb.2012.08.036>.
- [9] M.Z. Hashmi, M. Kaleem, U. Farooq, X. Su, P. Chakraborty, S.U. Rehman, Chemical remediation and advanced oxidation process of polychlorinated biphenyls in contaminated soils: a review, *Environ. Sci. Pollut. Control Ser.* (2022), <https://doi.org/10.1007/s11356-022-18668-3>.
- [10] Q. Huang, C.-S. Hong, TiO₂ photocatalytic degradation of PCBs in soil–water systems containing fluoro surfactant, *Chemosphere* 41 (2000) 871–879, [https://doi.org/10.1016/S0045-6535\(99\)00492-0](https://doi.org/10.1016/S0045-6535(99)00492-0).
- [11] I.W. Huang, C.S. Hong, B. Bush, Photocatalytic degradation of PCBs in TiO₂ aqueous suspensions, *Chemosphere* 32 (9) (1996) 1869–1881, [https://doi.org/10.1016/0045-6535\(96\)00080-x](https://doi.org/10.1016/0045-6535(96)00080-x).
- [12] E. Croom, Chapter three—metabolism of xenobiotics of human environments, in: E. Hodgson (Ed.), *Toxicology and Human Environments* vol 112, Academic Press, 2012, pp. 31–88, <https://doi.org/10.1016/B978-0-12-374741-1.ch003>.

- doi.org/10.1016/B978-0-12-415813-9.00003-9. Progress in Molecular Biology and Translational Science.
- [13] S. Sarkar, A. Banerjee, U. Halder, R. Biswas, R. Bandopadhyay, Degradation of synthetic azo dyes of textile industry: a sustainable approach using microbial enzymes, *Water Conserv. Sci. Eng.* 2 (4) (2017) 121–131, <https://doi.org/10.1007/s41101-017-0031-5>.
- [14] L.R.S. Pinheiro, D.G. Gradissimo, L.P. Xavier, A.V. Santos, Degradation of azo dyes: bacterial potential for bioremediation, *Sustainability* 14 (3) (2022), <https://doi.org/10.3390/su14031510>.
- [15] S.A. Zahran, M. Ali-Tammam, A.M. Hashem, R.K. Aziz, A.E. Ali, Azoreductase activity of dye-decolorizing bacteria isolated from the human gut microbiota, *Sci. Rep.* 9 (1) (2019) 5508, <https://doi.org/10.1038/s41598-019-41894-8>.
- [16] P. Suwannawong, S. Khammuang, R. Sarnthima, Decolorization of rhodamine B and congo red by partial purified laccase from *Lentinus polychrous* Lév, *J. Biochem. Technol.* 2 (3) (2010) 182–186.
- [17] M.M. Haque, M.A. Haque, M.K. Mosharaf, P.K. Marcus, Decolorization, degradation and detoxification of carcinogenic sulfonated azo dye methyl orange by newly developed biofilm consortia, *Saudi J. Biol. Sci.* 28 (1) (2021) 793–804, <https://doi.org/10.1016/j.sjbs.2020.11.012>.
- [18] M. Thakur, I.L. Medintz, S.A. Walper, Enzymatic bioremediation of organophosphate compounds—progress and remaining challenges, *Front. Bioeng. Biotechnol.* 7 (2019), <https://doi.org/10.3389/fbioe.2019.00289>.
- [19] M. Matula, T. Kucera, O. Soukup, J. Pejchal, Enzymatic degradation of organophosphorus pesticides and nerve agents by EC: 3.1.8.2, *Catalysts* 10 (12) (2020), <https://doi.org/10.3390/catal10121365>.
- [20] H. Mali, C. Shah, D.H. Patel, U. Trivedi, R.B. Subramanian, Degradation insight of organophosphate pesticide chlorpyrifos through novel intermediate 2,6-dihydroxypyridine by *Arthrobacter* sp. HM01, *Bioresour. Bioprocess.* 9 (1) (2022) 31, <https://doi.org/10.1186/s40643-022-00515-5>.
- [21] L. Ufarté, E. Laville, S. Duquesne, D. Morgavi, P. Robe, C. Klopp, et al., Discovery of carbamate degrading enzymes by functional metagenomics, *PLoS ONE* 12 (12) (2017) e0189201, <https://doi.org/10.1371/journal.pone.0189201>.
- [22] M. Umar Mustapha, N. Halimoon, W.L. Wan Johari, M.Y. Abd Shukor, Enhanced carbofuran degradation using immobilized and free cells of *Enterobacter* sp. isolated from soil, *Molecules* 25 (12) (2020), <https://doi.org/10.3390/molecules25122771>.
- [23] S. Ambreen, A. Yasmin, S. Aziz, Isolation and characterization of organophosphorus phosphatases from *Bacillus thuringiensis* MB497 capable of degrading Chlorpyrifos, Triazophos and Dimethoate, *Heliyon* 6 (7) (2020) e04221, <https://doi.org/10.1016/j.heliyon.2020.e04221>.
- [24] P. Pimviriyakul, T. Wongnate, R. Tinikul, P. Chaiyen, Microbial degradation of halogenated aromatics: molecular mechanisms and enzymatic reactions, *Microb. Biotechnol.* 13 (1) (2020) 67–86, <https://doi.org/10.1111/1751-7915.13488>.
- [25] F. Khalid, M.Z. Hashmi, N. Jamil, A. Qadir, M.I. Ali, Microbial and enzymatic degradation of PCBs from e-waste-contaminated sites: a review, *Environ. Sci. Pollut. Res. Int.* 28 (9) (2021) 10474–10487, <https://doi.org/10.1007/s11356-020-11996-2>.
- [26] S.F. Benitez, M.A. Sadañoski, J.E. Velázquez, P.D. Zapata, M.I. Fonseca, Comparative study of single cultures and a consortium of white rot fungi for polychlorinated biphenyls treatment, *J. Appl. Microbiol.* 131 (4) (2021) 1775–1786, <https://doi.org/10.1111/jam.15073>.
- [27] T. Steliga, K. Wojtowicz, P. Kapusta, J. Brzeszcz, Assessment of biodegradation efficiency of polychlorinated biphenyls (PCBs) and petroleum hydrocarbons (TPH) in soil using three individual bacterial strains and their mixed culture, *Molecules* 25 (3) (2020), <https://doi.org/10.3390/molecules25030709>.
- [28] M. Farhan, M. Ahmad, A. Kanwal, Z.A. Butt, Q.F. Khan, S.A. Raza, et al., Biodegradation of chlorpyrifos using isolates from contaminated agricultural soil, its kinetic studies, *Sci. Rep.* 11 (1) (2021) 10320, <https://doi.org/10.1038/s41598-021-88264-x>.
- [29] M. Ali, T.A. Naqvi, M. Kanwal, F. Rasheed, A. Hameed, S. Ahmed, Detection of the organophosphate degrading gene *OpdA* in the newly isolated bacterial strain *Bacillus pumilus* W1, *Ann. Microbiol.* 62 (1) (2012) 233–239, <https://doi.org/10.1007/s13213-011-0251-4>.
- [30] J. Germain, M. Raveton, M.N. Binet, B. Mouhamadou, Screening and metabolic potential of fungal strains isolated from contaminated soil and sediment in the polychlorinated biphenyl degradation, *Ecotoxicol. Environ. Saf.* 208 (2021) 111703, <https://doi.org/10.1016/j.ecoenv.2020.111703>.

- [31] S. Ahmed, M.G. Rasul, W.N. Martens, R. Brown, M.A. Hashib, Advances in heterogeneous photocatalytic degradation of phenols and dyes in wastewater: a review, *Water Air Soil Pollut.* 215 (1) (2011) 3–29, <https://doi.org/10.1007/s11270-010-0456-3>.
- [32] J.A. Coronado, Historical introduction to photocatalysis, *Green Energy Technol.* 71 (2013) 1–4, https://doi.org/10.1007/978-1-4471-5061-9_1.
- [33] A. Fujishima, K. Honda, Electrochemical photolysis of water at a semiconductor electrode, *Nature* 238 (5358) (1972) 37–38, <https://doi.org/10.1038/238037a0>.
- [34] D. Chen, Y. Cheng, N. Zhou, P. Chen, Y. Wang, K. Li, et al., Photocatalytic degradation of organic pollutants using TiO₂-based photocatalysts: a review, *J. Clean. Prod.* 268 (2020) 121725, <https://doi.org/10.1016/j.jclepro.2020.121725>.
- [35] M. Haque, D. Bahnemann, M. Muneer, Photocatalytic Degradation of Organic Pollutants: Mechanisms and Kinetics, 2012, <https://doi.org/10.5772/34522>.
- [36] S. Meenakshisundaram, Environmental photocatalysis/photocatalytic decontamination, in: L.M.T. Martínez, O.V. Kharissova, B.I. Kharisov (Eds.), *Handbook of Ecomaterials*, Springer International Publishing, Cham, 2019, pp. 1625–1640, https://doi.org/10.1007/978-3-319-68255-6_65.
- [37] V.-H. Nguyen, S.M. Smith, K. Wantala, P. Kajitvichyanukul, Photocatalytic remediation of persistent organic pollutants (POPs): a review, *Arab. J. Chem.* 13 (11) (2020) 8309–8337, <https://doi.org/10.1016/j.arabjc.2020.04.028>.
- [38] M.K.H.M. Nazri, N. Sapawe, A short review on photocatalytic toward dye degradation, *Mater. Today Proc.* 31 (2020) A42–A47, <https://doi.org/10.1016/j.matpr.2020.10.967>.
- [39] P.P. Morajkar, A.P. Naik, S.T. Bugde, B.R. Naik, Chapter 20—photocatalytic and microbial degradation of Amaranth dye, in: S.N. Meena, M.M. Naik (Eds.), *Advances in Biological Science Research*, Academic Press, 2019, pp. 327–345, <https://doi.org/10.1016/B978-0-12-817497-5.00020-3>.
- [40] A.P. Naik, A.V. Salkar, M.S. Majik, P.P. Morajkar, Enhanced photocatalytic degradation of Amaranth dye on mesoporous anatase TiO₂: evidence of C–N, N=N bond cleavage and identification of new intermediates, *Photochem. Photobiol. Sci.* 16 (7) (2017) 1126–1138, <https://doi.org/10.1039/C7PP00090A>.
- [41] C. Pragathiswaran, C. Smitha, B.M. Abbubakkar, P. Govindhan, N.A. Krishnan, Synthesis and characterization of TiO₂/ZnO–Ag nanocomposite for photocatalytic degradation of dyes and antimicrobial activity, *Mater. Today Proc.* 45 (2021) 3357–3364, <https://doi.org/10.1016/J.MATPR.2020.12.664>.
- [42] H. Deng, H. He, S. Sun, X. Zhu, D. Zhou, F. Han, et al., Photocatalytic degradation of dye by Ag/TiO₂ nanoparticles prepared with different sol–gel crystallization in the presence of effluent organic matter, *Environ. Sci. Pollut. Control Ser.* 26 (35) (2019) 35900–35912, <https://doi.org/10.1007/S11356-019-06728-0/FIGURES/11>.
- [43] X. Yu, J. Zhang, Y. Chen, Q. Ji, Y. Wei, J. Niu, et al., Ag–Cu₂O composite films with enhanced photocatalytic activities for methylene blue degradation: analysis of the mechanism and the degradation pathways, *J. Environ. Chem. Eng.* 9 (5) (2021) 106161, <https://doi.org/10.1016/J.JECE.2021.106161>.
- [44] Y. Li, F. Xiang, W. Lou, X. Zhang, MoS₂ with structure tuned photocatalytic ability for degradation of methylene blue, *IOP Conf. Ser. Earth Environ. Sci.* 300 (5) (2019) 052021, <https://doi.org/10.1088/1755-1315/300/5/052021>.
- [45] Z. Liang, R. Shen, Y.H. Ng, P. Zhang, Q. Xiang, X. Li, A review on 2D MoS₂ cocatalysts in photocatalytic H₂ production, *J. Mater. Sci. Technol.* 56 (2020) 89–121, <https://doi.org/10.1016/J.JMST.2020.04.032>.
- [46] S. Rashidi, S. Rashidi, R.K. Heydari, S. Esmaili, N. Tran, D. Thangi, W. Wei, WS₂ and MoS₂ counter electrode materials for dye-sensitized solar cells, *Prog. Photovolt. Res. Appl.* 29 (2) (2021) 238–261, <https://doi.org/10.1002/PIP.3350>.
- [47] Y. Wang, C. Yang, Y. Liu, Y. Fan, F. Dang, Y. Qiu, et al., Solvothermal synthesis of ZnO nanoparticles for photocatalytic degradation of methyl orange and P-nitrophenol, *Water (Basel)* 13 (22) (2021), <https://doi.org/10.3390/w13223224>.

- [48] H. He, X. Wang, C. Cheng, S. Yang, X. Wang, Q. Liu, et al., Degradation of organophosphorus flame retardant tri (chloro-propyl) phosphate (TCPP) by (001) crystal plane of TiO₂ photocatalysts, *Environ. Technol.* 42 (10) (2021) 1612–1622, <https://doi.org/10.1080/09593330.2019.1675771>.
- [49] K. Santhi, M. Navaneethan, S. Harish, S. Ponnusamy, C. Muthamizhchelvan, Synthesis and characterization of TiO₂ nanorods by hydrothermal method with different PH conditions and their photocatalytic activity, *Appl. Surf. Sci.* 500 (2020) 144058, <https://doi.org/10.1016/j.apsusc.2019.144058>.
- [50] W. Zuo, L. Zhang, Z. Zhang, S. Tang, Y. Sun, H. Huang, Y. Yu, Degradation of organic pollutants by intimately coupling photocatalytic materials with microbes: a review, *Crit. Rev. Biotechnol.* 41 (2) (2021) 273–299, <https://doi.org/10.1080/07388551.2020.1869689>.
- [51] S.S.R. Dasary, J. Saloni, A. Fletcher, Y. Anjaneyulu, H. Yu, Photodegradation of selected PCBs in the presence of nano-TiO₂ as catalyst and H₂O₂ as an oxidant, *Int. J. Environ. Res. Public Health* 7 (11) (2010) 3987–4001, <https://doi.org/10.3390/ijerph7113987>.
- [52] J. Zhao, T. Wu, K. Wu, K. Oikawa, H. Hidaka, N. Serpone, Photoassisted degradation of dye pollutants. 3. Degradation of the cationic dye rhodamine B in aqueous anionic surfactant/TiO₂ dispersions under visible light irradiation: evidence for the need of substrate adsorption on TiO₂ particles, *Environ. Sci. Technol.* 32 (16) (1998) 2394–2400, <https://doi.org/10.1021/es9707926>.
- [53] N. Neethu, T. Choudhury, Treatment of methylene blue and methyl orange dyes in wastewater by grafted titania pillared clay membranes, *Recent Pat. Nanotechnol.* 12 (3) (2018) 200–207, <https://doi.org/10.2174/1872210512666181029155352>.
- [54] A.P. Naik, H. Mittal, V.S. Wadi, L. Sane, A. Raj, S.M. Alhassan, et al., Super porous TiO₂ photocatalyst: tailoring the agglomerate porosity into robust structural mesoporosity with enhanced surface area for efficient remediation of azo dye polluted waste water, *J. Environ. Manage.* 258 (2020) 110029, <https://doi.org/10.1016/j.jenvman.2019.110029>.
- [55] A.P. Naik, J.V. Sawant, H. Mittal, A. Al Alili, P.P. Morajkar, Facile synthesis of 2D nanoflakes and 3D nanosponge-like Ni_{1-x}O via direct calcination of Ni (II) coordination compounds of Imidazole and 4-nitrobenzoate: adsorptive separation kinetics and photocatalytic removal of Amaranth dye contaminated wastewater, *J. Mol. Liq.* 325 (2021) 115235, <https://doi.org/10.1016/j.molliq.2020.115235>.
- [56] R. Gangadharachar, G.T. Chandrappa, Solution combustion synthesis of YVO₄ nanopowder using V₂O₅-NH₂O gel: photodegradation studies, *Trans. Indian Ceram. Soc.* 80 (1) (2021) 47–54, <https://doi.org/10.1080/0371750X.2020.1864664>.
- [57] P. Pascariu, C. Cojocaru, P. Samoila, A. Airinei, N. Oлару, D. Rusu, et al., Photocatalytic and antimicrobial activity of electrospun ZnO:Ag nanostructures, *J. Alloys Compd.* 834 (2020) 155144, <https://doi.org/10.1016/j.jallcom.2020.155144>.
- [58] J. López, A.A. Ortíz, F. Muñoz-Muñoz, D. Dominguez, J.N. Díaz de León, J.T.E. Galindo, et al., Magnetic nanostructured based on cobalt–zinc ferrites designed for photocatalytic dye degradation, *J. Phys. Chem. Solid.* 150 (2021) 109869, <https://doi.org/10.1016/j.jpcs.2020.109869>.
- [59] H. Sudrajat, S. Babel, Role of reactive species in the photocatalytic degradation of Amaranth by highly active N-doped WO₃, *Bull. Mater. Sci.* 40 (2017), <https://doi.org/10.1007/s12034-017-1502-1>.
- [60] M.A. Hamza, S.A. Abd El-Rahman, A.N. El-Shazly, E.M. Hashem, R.T. Mohamed, E.M. El-Tanany, M.G. Elmahgary, Facile one-pot ultrasonic-assisted synthesis of novel Ag@RGO/g-C₃N₄ ternary 0D@2D/2D nanocomposite with enhanced synergetic tandem adsorption-photocatalytic degradation of recalcitrant organic dyes: kinetic and mechanistic insights, *Mater. Res. Bull.* 142 (2021) 111386, <https://doi.org/10.1016/j.materresbull.2021.111386>.
- [61] C. Chandrashekar, P. Madhusudan, H.P. Shivaraju, S. Ponnappa, B. Basavalingu, S. Ananda, K. Byrappa, Synthesis of rare earth-doped yttrium vanadate polyscale crystals and their enhanced photocatalytic degradation of aqueous dye solution, *Int. J. Environ. Sci. Technol.* 15 (2017), <https://doi.org/10.1007/s13762-017-1401-4>.
- [62] M.-C. Rosu, M. Coros, F. Pogacean, L. Magerusan, C. Socaci, A. Turza, S. Pruneanu, Azo dyes degradation using TiO₂-Pt/graphene oxide and TiO₂-Pt/reduced graphene oxide photocatalysts under UV and natural sunlight irradiation, *Solid State Sci.* 70 (2017) 13–20, <https://doi.org/10.1016/j.solidstatesciences.2017.05.013>.

- [63] A. Khalil, N.M. Aboamera, W.S. Nasser, W.H. Mahmoud, G.G. Mohamed, Photodegradation of organic dyes by PAN/SiO₂-TiO₂-NH₂ nanofiber membrane under visible light, *Sep. Purif. Technol.* 224 (2019) 509–514, <https://doi.org/10.1016/j.seppur.2019.05.056>.
- [64] H.S.M. Abd-Rabboh, A.H. Galal, R.A. Aziz, M.A. Ahmed, A novel BiVO₃/SnO₂ step S-scheme nano-heterojunction for an enhanced visible light photocatalytic degradation of Amaranth dye and hydrogen production, *RSC Adv.* 11 (47) (2021) 29507–29518, <https://doi.org/10.1039/D1RA04717E>.
- [65] E.D. Mohamed Isa, N.W. Che Jusoh, R. Hazan, K. Shameli, Photocatalytic degradation of methyl orange using pullulan-mediated porous zinc oxide microflowers, *Environ. Sci. Pollut. Control Ser.* 28 (5) (2021) 5774–5785, <https://doi.org/10.1007/s11356-020-10939-1>.
- [66] F. Poorsajadi, M.H. Sayadi, M. Hajiani, M.R. Rezaei, Photocatalytic degradation of methyl orange dye using bismuth oxide nanoparticles under visible radiation, *Int. J. New Chem.* 8 (3) (2021) 229–239, <https://doi.org/10.22034/ijnc.2020.137235.1131>.
- [67] C. Jayakrishnan, S. Sheeja, J. Duraimurugan, S. Prabhu, R. Ramesh, G. Kumar, et al., Photoelectrochemical properties and photocatalytic degradation of methyl orange dye by different ZnO nanostructures, *J. Mater. Sci. Mater. Electron.* (2022), <https://doi.org/10.1007/s10854-022-07801-0>.
- [68] G. Liu, X. Pan, J. Li, C. Li, C. Ji, Facile preparation and characterization of anatase TiO₂/nanocellulose composite for photocatalytic degradation of methyl orange, *J. Saudi Chem. Soc.* 25 (12) (2021) 101383, <https://doi.org/10.1016/j.jscs.2021.101383>.
- [69] K.S. Kiran, S.V. Lokesh, Improved photocatalytic degradation of methyl orange dye in UV light irradiation by K₂Ti₆O₁₃ nanorods, *J. Turk. Chem. Soc. Sect. A Chem.* 8 (2021) 723–730, <https://doi.org/10.18596/jotcsa.766952>.
- [70] A. Singh, A. Ahmed, A. Sharma, C. Sharma, S. Paul, et al., Promising photocatalytic degradation of methyl orange dye via sol-gel synthesized Ag–CdS@Pr–TiO₂ core/shell nanoparticles, *Phys. B Condens. Matter* 616 (2021) 413121, <https://doi.org/10.1016/j.physb.2021.413121>.
- [71] V.Q. Hieu, T.K. Phung, T.-Q. Nguyen, A. Khan, V.D. Doan, V.A. Tran, V.T. Le, Photocatalytic degradation of methyl orange dye by Ti₃C₂–TiO₂ heterojunction under solar light, *Chemosphere* 276 (2021) 130154, <https://doi.org/10.1016/j.chemosphere.2021.130154>.
- [72] S.-G. Jeon, J.-W. Ko, W.-B. Ko, Ultrasound assisted synthesis of gadolinium oxide-zeolitic Imidazolate framework-8 nanocomposites and their optimization for photocatalytic degradation of methyl orange using response surface methodology, *Catalysts* 11 (9) (2021), <https://doi.org/10.3390/catal11091022>.
- [73] B.M. Phadi, O.A. Oyewo, S. Ramaila, L. Mavuru, D.C. Onwudiwe, Nanocomposite of CeVO₄/BiVO₄ loaded on reduced graphene oxide for the photocatalytic degradation of methyl orange, *J. Clust. Sci.* (2021), <https://doi.org/10.1007/s10876-021-02189-z>.
- [74] N. Wang, Z. Zhao, L. Liu, J. Xing, Preparation of muscovite/tungsten-doped TiO₂ composites for the efficient photocatalytic degradation of methyl orange under simulated solar light irradiation, *Inorg. Chem. Commun.* 138 (2022) 109285, <https://doi.org/10.1016/j.inoche.2022.109285>.
- [75] R. Shan, L. Lu, J. Gu, Y. Zhang, H. Yuan, Y. Chen, B. Luo, Photocatalytic degradation of methyl orange by Ag/TiO₂/biochar composite catalysts in aqueous solutions, *Mater. Sci. Semicond. Process.* 114 (2020) 105088, <https://doi.org/10.1016/j.mssp.2020.105088>.
- [76] C. Lin, J. Su, Z. Chen, S. Zhang, Q. Gong, Y. Qu, et al., Photocatalytic oxidative degradation of methyl orange by a novel g-C₃N₄@ZnO based on graphene oxide composites with ternary heterojunction construction, *React. Kinet. Mech. Catal.* (2022), <https://doi.org/10.1007/s11144-022-02200-2>.
- [77] V. Tran, K. Phung, V. Le, T. Vo, T.K. Vo, H. Vu-Quang, T. Nguyen, Solar-light-driven photocatalytic degradation of methyl orange dye over Co₃O₄-ZnO nanoparticles, *Mater. Lett.* (2020), <https://doi.org/10.1016/j.matlet.2020.128902>.
- [78] H. Yang, J. Yang, Photocatalytic degradation of rhodamine B catalyzed by TiO₂ films on a capillary column, *RSC Adv.* 8 (22) (2018) 11921–11929, <https://doi.org/10.1039/C8RA00471D>.

- [79] M. Ahmad, W. Rehman, M.M. Khan, M.T. Qureshi, A. Gul, S. Haq, et al., Phyto-genic fabrication of ZnO and gold decorated ZnO nanoparticles for photocatalytic degradation of rhodamine B, *J. Environ. Chem. Eng.* 9 (1) (2021) 104725, <https://doi.org/10.1016/j.jece.2020.104725>.
- [80] L. Mohanty, D. Sundar Pattanayak, R. Singhal, D. Pradhan, S. Kumar Dash, Enhanced photocatalytic degradation of rhodamine B and malachite green employing BiFeO₃/g-C₃N₄ nanocomposites: an efficient visible-light photocatalyst, *Inorg. Chem. Commun.* 138 (2022) 109286, <https://doi.org/10.1016/j.inoche.2022.109286>.
- [81] L.T.T. Nguyen, D.-V.N. Vo, L.T.H. Nguyen, A.T.T. Duong, H.Q. Nguyen, N.M. Chu, et al., Synthesis, characterization, and application of ZnFe₂O₄@ZnO nanoparticles for photocatalytic degradation of rhodamine B under visible-light illumination, *Environ. Technol. Innov.* 25 (2022) 102130, <https://doi.org/10.1016/j.eti.2021.102130>.
- [82] A. Singh, D. Singh, B. Ahmed, A.K. Ojha, Sun/UV-Light driven photocatalytic degradation of rhodamine B dye by Zn doped CdS nanostructures as photocatalyst, *Mater. Chem. Phys.* 277 (2022) 125531, <https://doi.org/10.1016/j.matchemphys.2021.125531>.
- [83] H. Ashiq, N. Nadeem, A. Mansha, J. Iqbal, M. Yaseen, M. Zahid, I. Shahid, G-C₃N₄/Ag@CoWO₄: a novel sunlight active ternary nanocomposite for potential photocatalytic degradation of rhodamine B dye, *J. Phys. Chem. Solid.* 161 (2022) 110437, <https://doi.org/10.1016/j.jpcs.2021.110437>.
- [84] X. Liu, J. Chen, L. Yang, S. Yun, M. Que, H. Zheng, et al., 2D/2D g-C₃N₄/TiO₂ with exposed (001) facets Z-scheme composites accelerating separation of interfacial charge and visible photocatalytic degradation of rhodamine B, *J. Phys. Chem. Solid.* 160 (2022) 110339, <https://doi.org/10.1016/j.jpcs.2021.110339>.
- [85] R. Kumar, A. Umar, R. Kumar, M. Chauhan, G. Kumar, S. Chauhan, Spindle-like Co₃O₄-ZnO nanocomposites scaffold for hydrazine sensing and photocatalytic degradation of rhodamine B dye, *Eng. Sci.* (2021), <https://doi.org/10.30919/es8d548>.
- [86] H. Widiyandari, N. Umiati, R. Herdianti, Synthesis and photocatalytic property of zinc oxide (ZnO) fine particle using flame spray pyrolysis method, *J. Phys. Conf. Ser.* 1025 (2018) 12004, <https://doi.org/10.1088/1742-6596/1025/1/012004>.
- [87] Y. Li, K.-A. Min, B. Han, L.Y.S. Lee, Ni nanoparticles on active (001) facet-exposed rutile TiO₂ nanopillar arrays for efficient hydrogen evolution, *Appl. Catal. B* 282 (2021) 119548, <https://doi.org/10.1016/j.apcatb.2020.119548>.
- [88] H. Mittal, A. Al Alili, P.P. Morajkar, S.M. Alhassan, GO crosslinked hydrogel nanocomposites of chitosan/carboxymethyl cellulose—a versatile adsorbent for the treatment of dyes contaminated wastewater, *Int. J. Biol. Macromol.* 167 (2021) 1248–1261, <https://doi.org/10.1016/J.IJBIOMAC.2020.11.079>.
- [89] H. Mittal, A. Al Alili, P.P. Morajkar, S.M. Alhassan, Graphene oxide crosslinked hydrogel nanocomposites of xanthan gum for the adsorption of crystal violet dye, *J. Mol. Liq.* 323 (2021) 115034, <https://doi.org/10.1016/J.MOLLIQ.2020.115034>.
- [90] H. Mittal, P.P. Morajkar, A. Al Alili, S.M. Alhassan, In-situ synthesis of ZnO nanoparticles using gum arabic based hydrogels as a self-template for effective malachite green dye adsorption, *J. Polym. Environ.* 28 (6) (2020) 1637–1653, <https://doi.org/10.1007/S10924-020-01713-Y/SCHEMES/2>.
- [91] J. Wang, T. Liu, J. Liu, X. Cao, J. Liu, Study on photocatalytic degradation of organophosphorus pesticides, *AIP Conf. Proc.* 2350 (1) (2021) 20031, <https://doi.org/10.1063/5.0048531>.
- [92] H. He, X. Wang, C. Cheng, S. Yang, X. Wang, Q. Liu, et al., Degradation of organophosphorus flame retardant tri (chloro-propyl) phosphate (TCPP) by (001) crystal plane of TiO₂ photocatalysts, *Environ. Technol.* 42 (2019) 1–36, <https://doi.org/10.1080/09593330.2019.1675771>.
- [93] A.H. Keihan, H. Rasoulnezhad, A. Mohammadgholi, S. Sajjadi, R. Hosseinzadeh, M. Farhadian, G. Hosseinzadeh, Pd nanoparticle loaded TiO₂ semiconductor for photocatalytic degradation of Paraoxon pesticide under visible-light irradiation, *J. Mater. Sci. Mater. Electron.* 28 (22) (2017) 16718–16727, <https://doi.org/10.1007/s10854-017-7585-z>.
- [94] A. Jonidi jafari, M. Gholami, M. Farzadkia, A. Esrafil, M. Shirzad-Siboni, Application of Ni-doped ZnO nanorods for degradation of diazinon: kinetics and by-products, *Sep. Sci. Technol.* 52 (2017), <https://doi.org/10.1080/01496395.2017.1303508>.

- [95] S. Nasser, M. Omidvar Borna, A. Esrafil, R. Rezaei Kalantary, B. Kakavandi, M. Sillanpää, A. Asadi, Photocatalytic degradation of malathion using Zn²⁺-doped TiO₂ nanoparticles: statistical analysis and optimization of operating parameters, *Appl. Phys. Mater. Sci. Process* 124 (2) (2018) 175, <https://doi.org/10.1007/s00339-018-1599-0>.
- [96] M. Aghaei, S. Sajjadi, A.H. Keihan, Sono-coprecipitation synthesis of ZnO/CuO nanophotocatalyst for removal of parathion from wastewater, *Environ. Sci. Pollut. Res. Int.* 27 (11) (2020) 11541–11553, <https://doi.org/10.1007/s11356-020-07680-0>.
- [97] Z. Zhu, F. Guo, Z. Xu, X. Di, Q. Zhang, Photocatalytic degradation of an organophosphorus pesticide using a ZnO/RGO composite, *RSC Adv.* 10 (20) (2020) 11929–11938, <https://doi.org/10.1039/D0RA01741H>.
- [98] R. Mansourian, S. Mousavi, S. Alizadeh, S. Sabbaghi, CeO₂/TiO₂/SiO₂ nanocatalyst for the photocatalytic and sonophotocatalytic degradation of chlorpyrifos, *Can. J. Chem. Eng.* (2021), <https://doi.org/10.1002/cjce.24157>.
- [99] M. Zhang, Y. Zhang, L. Tang, Y. Zhu, J. Wang, C. Feng, et al., Synergetic utilization of 3D materials merits and unidirectional electrons transfer of Schottky junction for optimizing optical absorption and charge kinetics, *Appl. Catal. B* 295 (2021) 120278, <https://doi.org/10.1016/j.apcatb.2021.120278>.
- [100] A. Saljooqi, T. Shamspur, A. Mostafavi, Synthesis and photocatalytic activity of porous ZnO stabilized by TiO₂ and Fe₃O₄ nanoparticles: investigation of pesticide degradation reaction in water treatment, *Environ. Sci. Pollut. Res. Int.* 28 (8) (2021) 9146–9156, <https://doi.org/10.1007/s11356-020-11122-2>.
- [101] S. Merci, A. Saljooqi, T. Shamspur, A. Mostafavi, Investigation of photocatalytic chlorpyrifos degradation by a new silica mesoporous material Immobilized by WS₂ and Fe₃O₄ nanoparticles: application of response surface methodology, *Appl. Organomet. Chem.* 34 (3) (2020) e5343, <https://doi.org/10.1002/aoc.5343>.
- [102] D. Majhi, Y.P. Bhoi, P.K. Samal, B.G. Mishra, Morphology controlled synthesis and photocatalytic study of novel CuS-Bi₂O₃CO₃ heterojunction system for chlorpyrifos degradation under visible light illumination, *Appl. Surf. Sci.* 455 (2018) 891–902, <https://doi.org/10.1016/j.apsusc.2018.06.051>.
- [103] F. Soltani-nezhad, A. Saljooqi, T. Shamspur, A. Mostafavi, Photocatalytic degradation of imidacloprid using GO/Fe₃O₄/TiO₂-NiO under visible radiation: optimization by response level method, *Polyhedron* 165 (2019) 188–196, <https://doi.org/10.1016/j.poly.2019.02.012>.
- [104] I. Manga Raju, T. Siva Rao, K.V. Divya Lakshmi, M. Ravi Chandra, J. Swathi Padmaja, G. Divya, Poly 3-thenoic acid sensitized, copper doped anatase/brookite TiO₂ nano hybrids for enhanced photocatalytic degradation of an organophosphorus pesticide, *J. Environ. Chem. Eng.* 7 (4) (2019) 103211, <https://doi.org/10.1016/j.jece.2019.103211>.
- [105] J. Li, B. Chu, Z. Xie, Y. Deng, Y. Zhou, L. Dong, et al., Mechanism and DFT study of degradation of organic pollutants on rare earth ions doped TiO₂ photocatalysts prepared by sol-hydrothermal synthesis, *Catal. Lett.* 152 (2) (2022) 489–502, <https://doi.org/10.1007/s10562-021-03634-4>.
- [106] A. Tomašević, A. Marinkovic, D. Mijin, M. Radisic, S. Porobic, N. Prlainović, S. Gasic, A study of photocatalytic degradation of methomyl and its commercial product Lannate-90, *Chem. Ind. Chem. Eng. Q.* 26 (2020) 2, <https://doi.org/10.2298/CICEQ190424002T>.
- [107] S. Huang, H. Tsai, J. Shaya, C.-S. Lu, Photocatalytic degradation of thiobencarb by a visible light-driven MoS₂ photocatalyst, *Sep. Purif. Technol.* 197 (2018), <https://doi.org/10.1016/j.seppur.2018.01.009>.
- [108] J. Zheng, W. Li, R. Tang, S. Xiong, D. Gong, Y. Deng, et al., Ultrafast photodegradation of Nitenpyram by Ag/Ag₃PO₄/Zn-Al LDH composites activated by persulfate system: removal efficiency, degradation pathway and reaction mechanism, *Chemosphere* 292 (2022) 133431, <https://doi.org/10.1016/j.chemosphere.2021.133431>.
- [109] C. Li, N. Wu, Y. Qi, J. Liu, X. Pan, J. Ge, et al., Preparation of nitrogen doped silica photocatalyst for enhanced photodegradation of polychlorinated biphenyls (PCB-209), *Chem. Eng. J.* 425 (2021) 131682, <https://doi.org/10.1016/j.cej.2021.131682>.
- [110] S. Safa, M.T. Ghaneian, M.H. Ehrampoush, Enhanced photocatalytic activity of efficient magnetically recyclable core-shell nanocomposites on 2,2',4,4',5,5'-hexachlorobiphenyl (PCB 153)

- degradation under UV-LED irradiation, *Environ. Sci. Pollut. Control Ser.* 28 (39) (2021) 54679–54694, <https://doi.org/10.1007/s11356-021-14202-z>.
- [111] A. ElMetwally, E. Zeynaloo, D. Shukla, B. Sumnar, S. Dhar, J. Cohn, et al., Cu₂O Cubes Decorated with Azine-Based Covalent Organic Framework Spheres and Pd Nanoparticles as Tandem Photocatalyst for Light-Driven Degradation of Chlorinated Biphenyls, 2021, <https://doi.org/10.1021/acsnm.0c03425>.
- [112] S. Khammar, N. Bahramifar, H. Younesi, Preparation and surface Engineering of CM-β-CD Functionalized Fe₃O₄@TiO₂ nanoparticles for photocatalytic degradation of polychlorinated biphenyls (PCBs) from transformer Oil, *J. Hazard Mater.* 394 (2020) 122422, <https://doi.org/10.1016/j.jhazmat.2020.122422>.
- [113] M. Yu, J. Wang, L. Tang, C. Feng, H. Liu, H. Zhang, et al., Intimate coupling of photocatalysis and biodegradation for wastewater treatment: mechanisms, recent advances and environmental applications, *Water Res.* 175 (2020) 115673, <https://doi.org/10.1016/J.WATRES.2020.115673>.
- [114] M.D. Marsolek, C.I. Torres, M. Hausner, B.E. Rittmann, Intimate coupling of photocatalysis and biodegradation in a photocatalytic circulating-bed biofilm reactor, *Biotechnol. Bioeng.* 101 (1) (2008) 83–92, <https://doi.org/10.1002/bit.21889>.
- [115] D. Zhou, Z. Xu, S. Dong, M. Huo, S. Dong, X. Tian, et al., Intimate coupling of photocatalysis and biodegradation for degrading phenol using different light types: visible light vs UV light, *Environ. Sci. Technol.* 49 (13) (2015) 7776–7783, https://doi.org/10.1021/ACS.EST.5B00989/SUPPL_FILE/ES5B00989_SI_001.PDF.
- [116] H. Xiong, D. Zou, D. Zhou, S. Dong, J. Wang, B.E. Rittmann, Enhancing degradation and mineralization of tetracycline using intimately coupled photocatalysis and biodegradation (ICPB), *Chem. Eng. J.* 316 (2017) 7–14, <https://doi.org/10.1016/J.CEJ.2017.01.083>.
- [117] G. Li, S. Park, B.E. Rittmann, Degradation of reactive dyes in a photocatalytic circulating-bed biofilm reactor, *Biotechnol. Bioeng.* 109 (4) (2012) 884–893, <https://doi.org/10.1002/BIT.24366>.
- [118] X. Zhang, Y. Wu, G. Xiao, Z. Tang, M. Wang, F. Liu, X. Zhu, Simultaneous photocatalytic and microbial degradation of dye-containing wastewater by a novel g-C₃N₄-P25/photosynthetic bacteria composite, *PLoS ONE* 12 (3) (2017), <https://doi.org/10.1371/JOURNAL.PONE.0172747> e0172747.
- [119] Z. Xing, W. Zhou, F. Du, Y. Qu, G. Tian, K. Pan, et al., A floating macro/mesoporous crystalline anatase TiO₂ ceramic with enhanced photocatalytic performance for recalcitrant wastewater degradation, *Dalton Trans.* 43 (2) (2013) 790–798, <https://doi.org/10.1039/C3DT52433G>.
- [120] J. Xiong, S. Guo, T. Zhao, Y. Liang, J. Liang, S. Wang, et al., Degradation of methylene blue by intimate coupling photocatalysis and biodegradation with bagasse cellulose composite carrier, *Cellulose* 27 (6) (2020) 3391–3404, <https://doi.org/10.1007/S10570-020-02995-0/FIGURES/10>.
- [121] N. Jafari, R. Kasra-Kermanshahi, M.R. Soudi, A.H. Mahvi, S. Gharavi, Degradation of a textile reactive azo dye by a combined biological-photocatalytic process: candida tropicalis Jks2-Tio2/Uv, *Iran. J. Environ. Health Sci. Eng.* 9 (1) (2012) 33, <https://doi.org/10.1186/1735-2746-9-33>.
- [122] S. Shoabargh, A. Karimi, G. Dehghan, A. Khataee, A hybrid photocatalytic and enzymatic process using glucose oxidase immobilized on TiO₂/polyurethane for removal of a dye, *J. Ind. Eng. Chem.* 20 (5) (2014) 3150–3156, <https://doi.org/10.1016/j.jiec.2013.11.058>.
- [123] T. Sharma, M. Kaur, A. Sobti, A. Rajor, A. Toor, Sequential microbial-photocatalytic degradation of imidacloprid, *Environ. Eng. Res.* 25 (2019) 597–604, <https://doi.org/10.4491/eer.2019.150>.
- [124] Y. Zhang, X. Pu, M. Fang, J. Zhu, L. Chen, B.E. Rittmann, 2,4,6-Trichlorophenol (TCP) photo-biodegradation and its effect on community structure, *Biodegradation* 23 (4) (2012) 575–583, <https://doi.org/10.1007/S10532-012-9534-0>.
- [125] G. Li, S. Park, D.W. Kang, R. Krajmalnik-Brown, B.E. Rittmann, 2,4,5-Trichlorophenol degradation using a novel TiO₂-coated biofilm carrier: roles of adsorption, photocatalysis, and biodegradation, *Environ. Sci. Technol.* 45 (19) (2011) 8359–8367, https://doi.org/10.1021/ES2016523/SUPPL_FILE/ES2016523_SI_001.PDF.
- [126] C. Zhang, L. Fu, Z. Xu, H. Xiong, D. Zhou, M. Huo, Contrasting roles of phenol and pyrocatechol on the degradation of 4-chlorophenol in a photocatalytic–biological reactor, *Environ. Sci. Pollut. Control Ser.* 24 (31) (2017) 24725–24731, <https://doi.org/10.1007/S11356-017-0245-2>.

- [127] Y. Liang, Q. Feng, J. Zhang, C. Jiao, J. Xiong, S. Wang, Q. Yang, Coupling of photocatalysis and biological treatment for elemental chlorine free bleaching wastewater: application of factorial design methodology, *J. Environ. Manage.* 302 (2022) 114111, <https://doi.org/10.1016/j.jenvman.2021.114111>.
- [128] F. Li, X. Lan, L. Wang, X. Kong, P. Xu, Y. Tai, et al., An efficient photocatalyst coating strategy for intimately coupled photocatalysis and biodegradation (ICPB): powder spraying method, *Chem. Eng. J.* 383 (2020) 123092, <https://doi.org/10.1016/j.cej.2019.123092>.
- [129] R. Ding, W. Yan, Y. Wu, Y. Xiao, H. Gang, S. Wang, et al., Light-excited photoelectrons coupled with bio-photocatalysis enhanced the degradation efficiency of oxytetracycline, *Water Res.* 143 (2018) 589–598, <https://doi.org/10.1016/j.watres.2018.06.068>.
- [130] H. Xiong, S. Dong, J. Zhang, D. Zhou, B.E. Rittmann, Roles of an easily biodegradable co-substrate in enhancing tetracycline treatment in an intimately coupled photocatalytic-biological reactor, *Water Res.* 136 (2018) 75–83, <https://doi.org/10.1016/j.watres.2018.02.061>.
- [131] Y. Ma, H. Xiong, Z. Zhao, Y. Yu, D. Zhou, S. Dong, Model-based evaluation of tetracycline hydrochloride removal and mineralization in an intimately coupled photocatalysis and biodegradation reactor, *Chem. Eng. J.* 351 (2018) 967–975, <https://doi.org/10.1016/j.cej.2018.06.167>.
- [132] Y. Wang, C. Chen, D. Zhou, H. Xiong, Y. Zhou, S. Dong, B.E. Rittmann, Eliminating partial-transformation products and mitigating residual toxicity of amoxicillin through intimately coupled photocatalysis and biodegradation, *Chemosphere* 237 (2019) 124491, <https://doi.org/10.1016/J.CHEMOSPHERE.2019.124491>.
- [133] D. Chi, D. Sun, Z. Yang, Z. Xing, Z. Li, Q. Zhu, W. Zhou, Bifunctional nest-like self-floating microreactor for enhanced photothermal catalysis and biocatalysis, *Environ. Sci. Nano* 6 (12) (2019) 3551–3559, <https://doi.org/10.1039/C9EN00968J>.
- [134] L. Zhang, Z. Xing, H. Zhang, Z. Li, X. Wu, X. Zhang, et al., High thermostable ordered mesoporous SiO₂-TiO₂ coated circulating-bed biofilm reactor for unpredictable photocatalytic and biocatalytic performance, *Appl. Catal. B* 180 (2016) 521–529, <https://doi.org/10.1016/J.APCATB.2015.07.002>.
- [135] M. Zhao, J. Shi, Z. Zhao, D. Zhou, S. Dong, Enhancing chlorophenol biodegradation: using a co-substrate strategy to resist photo-H₂O₂ stress in a photocatalytic-biological reactor, *Chem. Eng. J.* 352 (2018) 255–261, <https://doi.org/10.1016/j.cej.2018.07.018>.
- [136] G. Li, S. Park, B.E. Rittmann, Developing an efficient TiO₂-coated biofilm carrier for intimate coupling of photocatalysis and biodegradation, *Water Res.* 46 (19) (2012) 6489–6496, <https://doi.org/10.1016/J.WATRES.2012.09.029>.
- [137] M. Patela, V. Tsiridis, S. Kyriazis, P. Samaras, A. Kungolos, G.P. Sakellariopoulous, et al., Assessment, U. E. N. C. for E, Evaluation of Toxic Response of Heavy Metals and Organic Pollutants Using Microtox Acute Toxicity Test. Proceedings of the International Conference on Environmental Science and Technology 1, EPA, 2009, pp. 1200–1205.